

## Chapter 2

# Aerobic Metabolism and the Steady-State Concept

**Abstract** This chapter contains an analysis of the steady-state concept, as it is applied during light exercise. In this case, oxygen consumption increases upon exercise onset to attain a steady level, which can be maintained for a long period of time. The steady-state oxygen consumption is proportional to the exerted mechanical power. Under these circumstances, there is neither accumulation of lactate in blood nor changes in muscle phosphocreatine concentration: aerobic metabolism sustains the entire energy requirement of the exercising body. Once the steady state has been attained, the flow of oxygen is the same at all levels along the respiratory system. The quantitative relations determining the flow of oxygen across the alveoli and in blood are discussed. Special attention is given to the effects of ventilation—perfusion inequality and to the diffusion—perfusion interaction equations. The cardiovascular responses at exercise steady state are analysed in the context of the equilibrium between systemic oxygen delivery and systemic oxygen return. The relationship between oxygen consumption and power is discussed, along with the distinction between external and internal work during cycling. The concepts of mechanical efficiency of exercise and energy cost of locomotion are analysed. Concerning the latter, the distinction between aerodynamic work and frictional work is introduced. The roles of the cross-sectional surface area on the frontal plane and of air density in aerodynamic work are discussed. To end with, an equation linking ventilation, circulation and metabolism at exercise in a tight manner is developed, around the notion that the homeostasis of the respiratory system at exercise is maintained around given values of the constant oxygen return. This equation tells that, as long as we are during steady-state exercise in normoxia, any increase in the exercise metabolic rate requires an increase in ventilation that is proportional to that in oxygen consumption only if the pulmonary respiratory quotient stays invariant does not change, and an increase in cardiac output that is not proportional to the corresponding increase in oxygen consumption. At intense exercise, when lactate accumulation also occurs and hyperventilation superimposes, a new steady state would be attained only at  $P_A\text{CO}_2$  values lower than 40 mmHg: the homeostasis of the respiratory system would be modified. This new steady state, however, is never attained in fact, for reasons that are discussed in Chap. 3.

## Contents

Introduction .....	30
The Steady-State Concept .....	32
Quantitative Relationships at Steady State.....	33
The Effects of Ventilation—Perfusion Heterogeneity .....	37
Diffusion–Perfusion Interaction in Alveolar–Capillary Gas Transfer .....	43
Breathing Pure Oxygen and the Correction for Nitrogen.....	45
The Mechanical Efficiency of Exercise .....	46
Energy Cost of Locomotion .....	49
The Cardiovascular Responses to Exercise.....	54
The $\dot{Q} - \dot{V}O_2$ Diagram.....	55
Conclusions.....	59
References .....	60

## Introduction

The general theory of the energetics of muscular exercise looks at muscle as a biological engine, in which chemical energy—or metabolic energy—is transformed in mechanical work and heat. The ultimate step of this energy transformation is provided by ATP hydrolysis in the cross-bridge cycle. The low ATP concentration in muscle (on average 5 mmol per kg of wet muscle) requires continuous ATP resynthesis, which we owe to the ensemble of reactions comprised in the concept of intermediate metabolism. The detailed description of these reactions can be found in biochemistry textbooks, and the historical developments that led to them are summarized in Chap. 1. The general theory summarizes these reactions in three basic physiological concepts: aerobic metabolism, anaerobic lactic metabolism and anaerobic alactic metabolism. **Aerobic metabolism** includes the oxidation of glycogen and fatty acids to pyruvate and acetate, respectively, and their introduction into the Krebs cycle which feeds oxidative phosphorylation. It uses oxygen as oxidizer and has carbon dioxide as end product. **Anaerobic lactic metabolism** concerns the degradation of glycogen to pyruvate, with subsequent transformation in lactate. It occurs when the rate of energy transformation in the glycolytic pathway exceeds that of further oxidation of pyruvate in the Krebs cycle. **Anaerobic alactic metabolism** consists of the Lohmann's reaction. A qualitative representation of these concepts is shown in Fig. 2.1. A practical consequence of this picture of metabolism is that the rate at which metabolic energy is transformed by aerobic metabolism can be determined by a simple measure of oxygen consumption ( $\dot{V}O_2$ ). Similarly, the rate of lactate accumulation in blood ( $\dot{L}a$ ) is a measure of the rate of anaerobic lactic metabolism, and the rate at which phosphocreatine concentration varies in muscle ( $\dot{P}C$ ) defines the rate of anaerobic alactic metabolism.

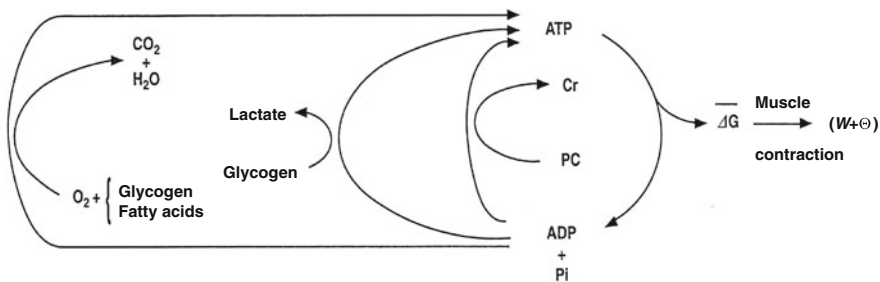


**Fig. 2.1** Schematic representation of the energetics of muscular exercise. ATP hydrolysis liberates the free energy ( $\Delta G$ ) that contractile proteins use to generate work ( $W$ ) and heat ( $\Theta$ ). ATP resynthesis takes place through the indicated pathways. *ADP* adenosine di-phosphate; *Pi* inorganic phosphate; *PC* phosphocreatine; *Cr* creatine. Modified after di Prampero (1985)

The quantitative representation of the same concepts takes the following algebraic form:

$$\dot{E} \propto \overleftarrow{ATP} = \overrightarrow{ATP} = c \dot{V} O_2 + b \dot{L}a + a \dot{P}C \quad (2.1)$$

where  $\overleftarrow{ATP}$  and  $\overrightarrow{ATP}$  are the rates of ATP hydrolysis and resynthesis, respectively. Equation (2.1) can be defined as the **general equation of the energetics of muscular exercise**. In this equation,  $\dot{E}$  is the overall rate of metabolic energy liberation, whereas the three constants  $a$ ,  $b$  and  $c$  are proportionality constants indicating the moles of ATP resynthesized, respectively, by a mole of phosphocreatine hydrolysed, a mole of lactate accumulated, and a mole of oxygen consumed. The Lohmann's reaction tells that  $a$  is equal to 1;  $c$  (otherwise  $P/O_2$  ratio) takes a mean value of 6.17 for glycogen oxidation into glycolysis. For constant  $b$ , the situation is a bit more complex than this (di Prampero 1981; di Prampero and Ferretti 1999) and will be discussed in Chap. 6.

In humans at rest and during light exercise,  $\dot{V} O_2$  attains a steady level which can be maintained for a long period of time. Under these steady-state conditions, there is neither accumulation of lactate in blood nor changes in muscle phosphocreatine concentration. Thus, Eq. (2.1) reduces to the following:

$$\dot{E} \propto \overleftarrow{ATP} = \overrightarrow{ATP} = c \dot{V} O_2 \quad (2.2)$$

Equation (2.2) indicates that all energy-sustaining body functions at rest plus the mechanical work of exercise derives from aerobic energy sources. This represents a particularly favourable condition for exercise physiologists, because a simple measure of  $\dot{V} O_2$  at the mouth informs on the overall metabolic power, which remains invariant in time.

In this chapter, I will discuss the steady-state concept and describe the quantitative relationships that characterize it. Making use of the steady-state concept,

I will then introduce the concepts of energy cost of locomotion and of mechanical efficiency of exercise. Finally, I will present and discuss the cardiopulmonary responses to exercise at steady state, and I will propose a synthesis of the inter-related phenomena along the respiratory system by which a steady  $\dot{V}O_2$  is maintained throughout the exercise.

## The Steady-State Concept

The steady-state concept was clearly defined for the first time by Bock et al. (1928). According to them, a steady state implies an invariant  $\dot{V}O_2$ , a steady rate of elimination of carbon dioxide ( $\dot{V}CO_2$ ) produced by metabolism only, steady heart rate ( $f_h$ ) and an essentially stable internal environment. If this is so, then (i) the  $\dot{V}O_2$  measured at the mouth corresponds to the rate of oxygen consumption by the mitochondria; (ii) both  $\dot{V}O_2$  and  $\dot{V}CO_2$  are characterized by equal values at any level along the respiratory system; (iii) as a consequence, the respiratory quotient determined at the lungs ( $RQ_L$ )—or gas exchange ratio, defined as the ratio between  $\dot{V}CO_2$  and  $\dot{V}O_2$ —is equal at any level along the respiratory system, so that it corresponds exactly to the metabolic respiratory quotient ( $RQ_M$ ), that is, the ratio between the moles of carbon dioxide produced and the moles of oxygen consumed in the cellular aerobic energy transformation processes. Starting from these bases, taken as axioms, several developments in the analysis of the quantitative relationships describing gas flows in the respiratory system at rest and exercise were pursued.

Before entering into these details, however, it is necessary to point out that the steady-state concept is a mental creation of some bright physiologists, which represents an oversimplification of what actually occurs in a living organism. In fact, even at steady state, the respiratory system is characterized by oxygen flow discontinuities, heterogeneities and spontaneous variations, depending on the macroscopic and microscopic organization of the system itself. From the macroscopic viewpoint, note that ventilation occurs in a dead-end pathway, so that inhalation and exhalation occur necessarily in alternate manner. Moreover, the heart alternates systoles and diastoles, with associated opening and closing of heart valves. Both mechanisms are sources of discontinuities, the former in air, the latter in blood flow, both in oxygen flow. Moreover, there is a spontaneous variability of respiratory and cardiac rhythms, related to mechanical and neural control mechanisms (Cottin et al. 2008; Perini and Veicsteinas 2003). This being the case, the  $\dot{V}O_2$  at steady state is not a continuous invariant flow: it rather corresponds to an invariant integral mean of a flow that is highly variable in time, at several levels even discontinuous.

From the microscopic viewpoint, blood flow is pulsatile in lung capillaries, because of their heterogeneous recruitment, and of interferences from the rhythmic activity of the heart and the lungs (Baumgartner et al. 2003; Clark et al. 2011; Tanabe et al. 1998). This heterogeneity may be reduced during exercise due to

simultaneous recruitment of a larger number of lung capillaries. Similar heterogeneities have been demonstrated also in contracting skeletal muscles, both in space and in time (Armstrong et al. 1987; Ellis et al. 1994; Heinonen et al. 2007; Marconi et al. 1988; Piiper et al. 1985). Heterogeneous muscle blood flow was reported also in non-contracting muscles of exercising humans (Heinonen et al. 2012). Contracting muscle fibres are likely unperfused, because they generate pressure, which compresses and closes muscle capillaries from outside. If this is so, perfusion occurs only in relaxing muscle fibres, so that muscle fibre oxygenation takes place during relaxation, not during contraction. In this case, the alternate recruitment of neighbouring motor units becomes a functional necessity, the inevitable consequence of which is heterogeneity of muscle blood flow distribution during muscular work.

## Quantitative Relationships at Steady State

The first relationships to be established in time concern the net amount of gas exchanged in the lungs and in blood, calculated as difference between a flow in and a flow out for the gas at stake. Concerning blood, this gave origin to what is nowadays called the **Fick principle**, whose algebraic expression is as follows (Fick 1870):

$$\dot{V} O_2 = \dot{Q} CaO_2 - \dot{Q} C\bar{v}O_2 = \dot{Q} (CaO_2 - C\bar{v}O_2) \quad (2.3)$$

where  $\dot{Q}$  is total blood flow—or more commonly **cardiac output**—and  $CaO_2$  and  $C\bar{v}O_2$  are the oxygen concentrations in arterial and mixed venous blood, respectively. This expression in fact defines the amount of oxygen that leaves the blood in peripheral capillaries to be consumed in cells in a unit of time. By analogy, Geppert and Zuntz (1888) defined  $\dot{V} O_2$  as the difference between inspired and expired oxygen flows, as follows:

$$\dot{V} O_2 = \dot{V}_I F_I O_2 - \dot{V}_E F_E O_2 \quad (2.4)$$

where  $\dot{V}_I$  is the total inspired air flow—or more commonly inspiratory ventilation;  $\dot{V}_E$  is the total expired air flow—or more commonly expiratory ventilation; and  $F_I O_2$  and  $F_E O_2$  are the oxygen fractions in inspired and expired air, respectively. By definition, at steady state, Eqs. (2.3) and (2.4) have equal solutions.

Similar equations can be written to define  $\dot{V} CO_2$ , by replacing its concentrations in blood—or its fractions in air—for the corresponding concentrations or fractions of oxygen. It is noteworthy, however, that the carbon dioxide concentration is higher in alveolar than in inspired air, and in mixed venous than in arterial blood, so that  $\dot{V} CO_2$  turns out negative. This being so, we have in blood:

$$\dot{V} \text{CO}_2 = \dot{Q} Ca\text{CO}_2 - \dot{Q} C\bar{v}\text{CO}_2 = \dot{Q} (Ca\text{CO}_2 - C\bar{v}\text{CO}_2) \quad (2.5)$$

where  $Ca\text{CO}_2$  and  $C\bar{v}\text{CO}_2$  are the carbon dioxide concentrations, respectively, in arterial and mixed venous blood. It is of note that, in spite of its negative values, it soon became customary to express  $\dot{V} \text{CO}_2$  as absolute value, making abstraction of the sign.

Considering alveolar air, since in respiration physiology the carbon dioxide fraction in inspired air is considered nil,  $\dot{V} \text{CO}_2$  computation turns out simplified, as follows:

$$\dot{V} \text{CO}_2 = -\dot{V}_E F_E \text{CO}_2 = -\dot{V}_A F_A \text{CO}_2 = -\dot{V}_A \frac{P_A \text{CO}_2}{P_B} \quad (2.6)$$

where  $\dot{V}_A$  is alveolar ventilation,  $F_A \text{CO}_2$  and  $P_A \text{CO}_2$  are the fraction and partial pressure, respectively, of carbon dioxide in alveolar air, and  $P_B$  is the barometric pressure. Equation (2.6) demonstrates that at any given  $P_B$  and  $\dot{V} \text{CO}_2$ ,  $\dot{V}_A$  is inversely proportional to  $P_A \text{CO}_2$ , whereas at any given  $P_A \text{CO}_2$ , it is directly proportional to  $\dot{V} \text{CO}_2$ . The former relationship is reported in Fig. 2.2a. The latter relationship, which appears in Fig. 2.2b, is stable on a precise  $P_A \text{CO}_2$  isopleth (that for  $P_A \text{CO}_2 = 40$  mmHg) as long as a “true” steady state is maintained. This is so if there is no accumulation of lactate in blood. On ordinary non-athletic individuals, blood lactate accumulation starts having an impact on pH regulation at powers corresponding to some two-thirds of the maximal aerobic power. Although the exercise is still submaximal, above this power pH is not sufficiently buffered, hyperventilation superimposes and the  $\dot{V}_A$  versus  $\dot{V} \text{CO}_2$  relationship bends upwards—higher  $\dot{V}_A/\dot{V} \text{CO}_2$  ratio and lower  $P_A \text{CO}_2$ : the steady-state condition is broken. The origin of lactate in steady-state submaximal exercise is discussed in Chap. 3. It is nonetheless noteworthy already at this stage that the buffering of lactic acidosis in these circumstances has nothing to do with the concept, unfortunately deeply rooted in sport science, of shifting from aerobic to anaerobic metabolism.

If we express Eq. (2.4) in terms of partial pressures of alveolar gases, and we combine Eqs. (2.4) and (2.6) in the definition of  $RQ_L$ , we obtain

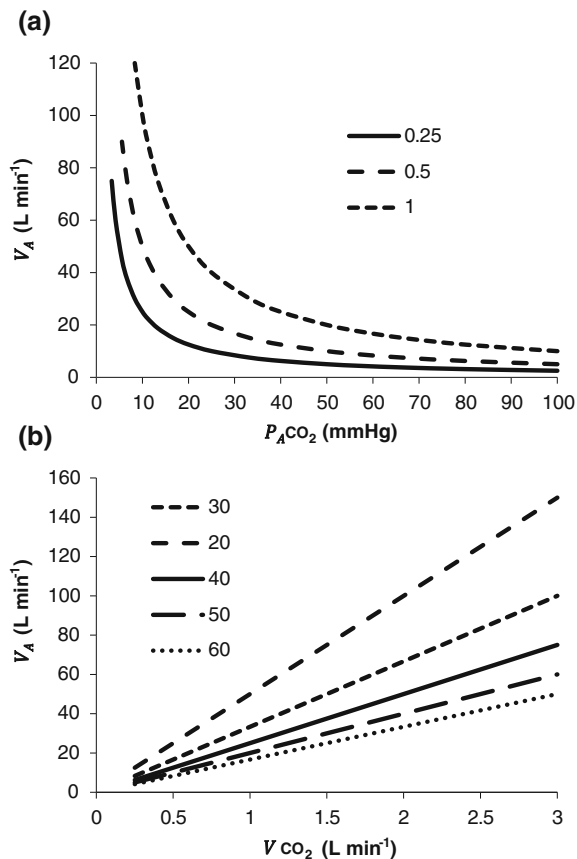
$$RQ_L = \frac{-P_A \text{CO}_2}{(P_I \text{O}_2 - P_A \text{O}_2)} \quad (2.7)$$

where  $P_L \text{O}_2$  is the oxygen partial pressure in inspired air. The solution of Eq. (2.7) for  $P_A \text{O}_2$  and  $P_A \text{CO}_2$  is

$$P_A \text{O}_2 = P_I \text{O}_2 - \frac{P_A \text{CO}_2}{-RQ_L} \quad (2.8a)$$

$$P_A \text{CO}_2 = RQ_L (P_A \text{O}_2 - P_I \text{O}_2) \quad (2.8b)$$

**Fig. 2.2** *Panel a* Inverse relationship between alveolar ventilation ( $\dot{V}_A$ ) and alveolar partial pressure of carbon dioxide ( $P_A\text{CO}_2$ ) at the three indicated levels of steady-state carbon dioxide flow ( $\dot{V}\text{CO}_2$ , in  $\text{L min}^{-1}$ ). *Panel b* Direct relationship between  $\dot{V}_A$  and  $\dot{V}\text{CO}_2$  at the indicated levels of  $P_A\text{CO}_2$  (in mmHg)



These equations are algebraic expressions of what is generally called the **alveolar air equation**. Its graphical representation is the  **$\text{O}_2\text{--CO}_2$  diagram for alveolar gases** (Rahn and Fenn 1955, see Fig. 2.3a), wherein we plot  $P_A\text{CO}_2$  on the y-axis and  $P_A\text{O}_2$  on the x-axis. Equation (2.8b) tells that there is a linear relationship between these two variables, with negative slope equal to  $-RQ_L$  and x-axis intercept corresponding to the inspired air composition, with  $P_A\text{CO}_2 = 0$  mmHg and  $P_A\text{O}_2 = P_I\text{O}_2$ . A family of isopleths for  $RQ_L$ , all converging on a given inspired air composition (e.g.  $P_I\text{O}_2 = 150$  mmHg at sea level), can be constructed. At steady state, the only possible combinations of  $P_A\text{CO}_2$  and  $P_A\text{O}_2$  are those that lie on the  $RQ_L$  isopleth corresponding to the actual  $RQ_M$ . For any metabolic level below the critical power (see Chap. 5), the  $\dot{V}_A/\dot{V}\text{CO}_2$  ratio is about 20 and the  $P_A\text{CO}_2$  is about 40 mmHg, whereas the steady-state  $P_A\text{O}_2$  would vary depending on  $RQ_L$ . Of course,  $P_I\text{O}_2$  decreases in hypoxia and increases in hyperoxia, so that the inspired air point is accordingly shifted leftwards and rightwards, respectively, and so is the entire family of  $RQ_L$  isopleths converging on it. In spite of this, as long as the metabolic rate stays below the critical power or the anaerobic threshold and there is no hyperventilation

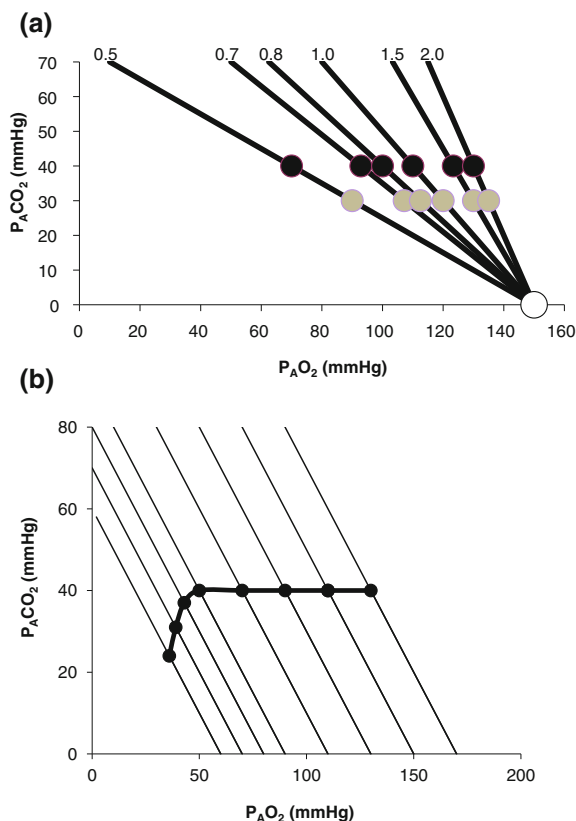


**Fig. 2.3** *Panel a* An  $\text{O}_2$ – $\text{CO}_2$  diagram for alveolar air on which six isopleths of pulmonary respiratory quotient are indicated, all converging on the inspired air point corresponding to sea level (barometric pressure of 760 mmHg, white dot). On each isopleth, the points corresponding to alveolar air composition (black dots) and expired air composition (grey dots) are also shown. *Panel b* An  $\text{O}_2$ – $\text{CO}_2$  diagram for alveolar air, on which eight parallel isopleths (thin lines), corresponding to a pulmonary respiratory quotient of 1.0, are indicated, converging on different inspired air points. The lower is the inspired partial pressure of oxygen, the more the isopleth is displaced to the left. The corresponding alveolar air compositions are also shown (black dots) and connected by the alveolar air curve (thick black curve)

consequent to hypoxaemic stimulation of peripheral chemoreceptors, the  $\dot{V}_A/\dot{V}\text{CO}_2$  ratio remains about 20, and the steady-state  $P_A\text{CO}_2$  remains equal to 40 mmHg. Conversely, as hyperventilation appears, e.g., due to ventilatory response to hypoxaemia, the  $\dot{V}_A/\dot{V}\text{CO}_2$  ratio increases and, since it is inversely proportional to  $P_A\text{CO}_2$ , this decreases, moving downwards and rightwards along the corresponding  $R_{Q_L}$  isopleth, in the direction of the inspired air point. If at all  $P_{I\text{O}_2}$  values we connect all the points representing the steady-state alveolar air composition, we obtain a curve like that reported in Fig. 2.3b, which is generally called the **normal mean alveolar air curve**.



Equation (2.7) is a particular case in which nitrogen balance is nil, which is the case only when  $RQ_L = -1$ . A resting human at steady state takes up 300 ml of oxygen per minute and gives out 250 ml of carbon dioxide per minute, on average, so that his  $RQ_L$  is equal to  $-0.83$ . This means that inspired ventilation, or the air flow inside the alveoli, is higher than expired ventilation, because there is less carbon dioxide that is added to alveolar air than oxygen that is subtracted. Since pressure must equilibrate, this implies that inert gases, namely nitrogen, compensate for pressure differences. Thus, when  $RQ_L \neq -1$ , Eq. (2.7) becomes

$$RQ_L = \frac{-P_A\text{CO}_2}{\left(P_I\text{O}_2 \cdot \frac{P_A\text{N}_2}{P_I\text{N}_2} - P_A\text{O}_2\right)} \quad (2.9)$$

The two theoretical extremes for possible variations of  $RQ_L$  are represented by  $RQ_L = 0$  and  $RQ_L = -\infty$ . The former is the case when  $\dot{V}\text{CO}_2$  is nil, the latter when  $\dot{V}\text{O}_2$  is nil. In the former case, since there is no carbon dioxide addition to the alveoli,  $P_A\text{CO}_2 = 0$  mmHg : the corresponding isopleth for  $RQ_L$  coincides with the  $x$ -axis. In the latter case, we have carbon dioxide addition to the alveoli in the absence of oxygen uptake: in this condition, there is a progressive dilution of oxygen and nitrogen in carbon dioxide, which goes on until carbon dioxide becomes the only alveolar gas. In this case,  $F_A\text{CO}_2 = 1$  and  $P_A\text{CO}_2 = 713$  mmHg at sea level. As a consequence, the corresponding isopleth for  $RQ_L$  does not coincide with the  $y$ -axis, but connects the point on the  $x$ -axis corresponding to inspired air composition to the point on the  $y$ -axis representing  $P_A\text{CO}_2 = 713$  mmHg.

## The Effects of Ventilation—Perfusion Heterogeneity

Although the  $\text{O}_2$ – $\text{CO}_2$  diagram was established for alveolar air, a similar diagram can be constructed for blood, starting from the computation of the respiratory quotient for blood ( $RQ_B$ ) after Eqs. (2.3) and (2.5):

$$RQ_B = \frac{(\text{CaCO}_2 - \bar{C}\bar{v}\text{CO}_2)}{(\text{CaO}_2 - \bar{C}\bar{v}\text{O}_2)} \quad (2.10)$$

from which we obtain the following solution for  $\text{CaCO}_2$ :

$$\text{CaCO}_2 = \bar{C}\bar{v}\text{CO}_2 - RQ_B(\text{CaO}_2 - \bar{C}\bar{v}\text{O}_2) \quad (2.11)$$

Equation (2.11), which is called the **arterial blood equation**, tells that, if we plot  $\text{CaCO}_2$  as a function of  $\text{CaO}_2$ , we obtain a family of straight lines, with negative slopes equal to  $RQ_B$ , which converge on a point, whose coordinates define the respiratory gas composition of mixed venous blood (Fig. 2.4). This means that,

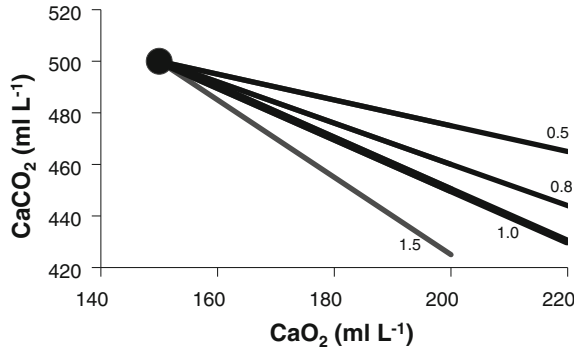


**Fig. 2.4** Carbon dioxide concentration in arterial blood ( $\text{CaCO}_2$ ) as a function of oxygen concentration of arterial blood ( $\text{CaO}_2$ ). The large dot refers to the concentrations occurring in mixed venous blood, where the isopleths for blood respiratory quotient (four of them are reported on the Figure, for the indicated values of respiratory quotient) converge

if no gas exchange occurs in the lungs, arterial blood would have the same oxygen and carbon dioxide concentrations as mixed venous blood.

Respiratory gases move across the alveolar–capillary barrier by diffusion, driven by differences in partial pressure, not in concentration, which is dictated by the binding characteristics of respiratory gases to haemoglobin. So, it would have some interest expressing Eq. (2.11) in terms of partial pressures:

$$\beta_c P_a \text{CO}_2 = \beta_c P_v \text{CO}_2 - RQ_B \beta_b (P_a \text{O}_2 - P_v \text{O}_2) \quad (2.12)$$

where constants  $\beta_c$  and  $\beta_b$  are the blood transport coefficients of carbon dioxide and oxygen, respectively, i.e. the slopes of the respective equilibrium curves with haemoglobin. The segment of the carbon dioxide equilibrium curve corresponding to the physiological range is practically linear, so that  $\beta_c$  can be taken as invariant. In contrast, this is not so for  $\beta_b$ : due to the shape of the oxygen equilibrium curve,  $\beta_b$  is lower the higher is the  $P\text{O}_2$ . An analytical solution of Eq. (2.12) thus requires an *a priori* solution of the oxygen equilibrium curve.

All models describing the oxygen equilibrium curve are empirical, except Hill's logarithmic model (Hill 1910; Ferretti 2012), whose theoretical basis, however, was confuted by the demonstration of the stereochemistry of haemoglobin (Perutz 1970). Although more precise descriptions of the oxygen equilibrium curve were published afterwards, Hill's model has the great advantage of simplicity, while remaining accurate enough for the purpose of constructing an analytical solution of Eq. (2.12). This solution is presented in Fig. 2.5, which is generally called the **O<sub>2</sub>–CO<sub>2</sub> diagram for blood gases** (Rahn and Fenn 1955). This plot describes a family of curves, whose shape is dictated by the value that  $\beta_b$  takes at any  $P\text{O}_2$ . All these curves converge on a point, whose coordinates define the respiratory gas partial pressures of mixed venous blood.

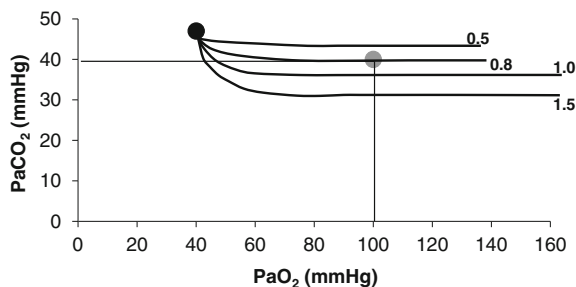


**Fig. 2.5** An  $O_2$ – $CO_2$  diagram for blood on which four isopleths of blood respiratory quotient are indicated, all converging on the mixed venous blood point (black dot). The grey dot refers to the arterial blood gas composition of a man at rest (respiratory quotient of 0.8).  $P_{aCO_2}$  is the partial pressure of carbon dioxide in arterial blood;  $P_{aO_2}$  is the partial pressure of oxygen in arterial blood

At steady state,  $RQ_B = RQ_L$ . If pulmonary gas exchange is complete, and equilibrium is attained on either side of the alveolar–capillary barrier, then arterial blood and alveolar air should have equal oxygen and carbon dioxide partial pressures. This coincidence of partial pressure values must then occur at the same respiratory quotient. Superposition on the same plot of the  $O_2$ – $CO_2$  diagrams for blood gases and for alveolar air (Fig. 2.6) clearly shows that this occurs at the crossing of two isopleths for a given  $RQ_B$  and  $RQ_L$  value (Farhi and Rahn 1955).

Figure 2.6 implies that (i) at any given respiratory quotient, only one combination of oxygen and carbon dioxide partial pressures is in fact possible, if we admit  $P_{AO_2} = P_{aO_2}$  (ideal air, as defined by Farhi and Rahn 1955); (ii) this combination is comprised between two extremes, one represented by  $P_{AO_2} = P_{vO_2}$ , the other by  $P_{AO_2} = P_{iO_2}$ ; and (iii) connecting all possible combinations of oxygen and carbon dioxide partial pressures at steady state leads to the construction of a curve called

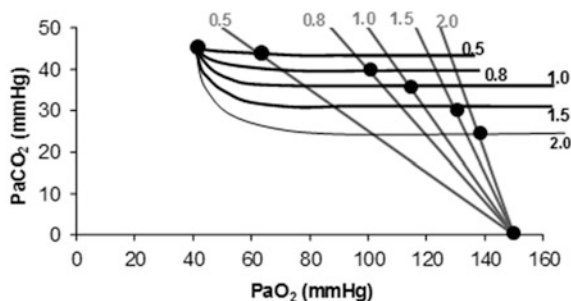


**Fig. 2.6** Construction of the ideal air curve on an  $O_2$ – $CO_2$  diagram. The respiratory quotient isopleths for alveolar air are in grey, the corresponding isopleths for blood are in black. Dots are located at the crossing of each couple of isopleths and on the two extremes: the mixed venous blood composition (upper left dot) and the inspired air composition (lower right dot). The ideal air curve connects all these dots from mixed venous blood to inspired air

the **ideal air curve**. It is of note that also the ideal air curve reflects the characteristics of the oxygen equilibrium curve: at high  $PO_2$ , when we operate on the flat part of the latter curve and we hyperventilate, relatively large drops of  $PCO_2$  are associated with small increases in  $PO_2$ ; conversely, in the low  $PO_2$  range, when we operate on the steep part of the oxygen equilibrium curve, relatively small increases of  $PCO_2$  are associated with large drops in  $PO_2$ .

If we solve Eq. (2.6) for  $\dot{V}_A$ , we have

$$\dot{V}_A = -\frac{\dot{V}CO_2}{F_ACO_2} \quad (2.13)$$

$\dot{V}_A$  and  $\dot{V}CO_2$  are not expressed in the same condition, since by convention the former is expressed in BTPS and the latter in STPD. Thus, if, after correcting for this inconsistency, we merge all constants and we transform  $F_ACO_2$  in  $P_ACO_2$  by means of Dalton's law, we obtain

$$\dot{V}_A = -\frac{(Pb - 47)\dot{V}CO_2}{CgP_ACO_2} \quad (2.14)$$

where  $Cg$  is the merged constant for STPD–BTPS transformation (0.863). If we replace  $\dot{V}O_2$  for  $\dot{V}CO_2$  in Eq. (2.14), we get

$$\dot{V}_A = -\frac{CgRQ_L\dot{V}O_2}{P_ACO_2} \quad (2.15)$$

whence

$$\dot{V}O_2 = -\frac{\dot{V}_A P_ACO_2}{CgRQ_L} \quad (2.16)$$

At steady state, since  $\dot{V}O_2$  is the same at all levels along the respiratory system, Eqs. (2.16) and (2.3) must provide equivalent  $\dot{V}O_2$  values, so that, when we take their ratio, we have

$$-\frac{\dot{V}_A P_ACO_2}{CgRQ_L\dot{Q}(CaO_2 - C\bar{v}O_2)} = 1 \quad (2.17)$$

whence, after rearrangement, we get

$$\frac{\dot{V}_A}{\dot{Q}} = -\frac{CgRQ_L(CaO_2 - C\bar{v}O_2)}{P_ACO_2} \quad (2.18)$$

which Hermann Rahn and Wallace Fenn called the **ventilation–perfusion equation** (Rahn and Fenn 1955). Equation (2.18) tells that at steady state, in any given

segment of the lungs, the  $\frac{\dot{V}_A}{\dot{Q}}$  ratio is directly proportional to  $-RQ_L$  and to  $(CaO_2 - C\bar{v}O_2)$  and inversely proportional to  $P_A CO_2$ . As a consequence, on the ideal air curve (Fig. 2.6), each point corresponds not only to a specific  $RQ_L$  value, but also to a unique value of  $\frac{\dot{V}_A}{\dot{Q}}$  ratio, which is lower the closer is  $RQ_L$  to zero. Moreover, if we look at the extremes of the ideal air curve, we note that, when  $\frac{\dot{V}_A}{\dot{Q}} = 0$ ,  $(CaO_2 - C\bar{v}O_2) = 0 \text{ ml L}^{-1}$ , so that the blood that leaves alveolar capillaries in which  $\frac{\dot{V}_A}{\dot{Q}} = 0$  has the same composition of mixed venous blood. On the other side, whenever  $\frac{\dot{V}_A}{\dot{Q}} = \infty$ ,  $P_A CO_2 = 0 \text{ mmHg}$ , so that the composition of alveolar air becomes equal to that of inspired air.

During light exercise at steady state, as compared to rest,  $\dot{V}_A$  increases in direct proportion to  $-\dot{V} CO_2$ , whereas the increase of  $\dot{Q}$  is less. As a consequence, the  $\frac{\dot{V}_A}{\dot{Q}}$  ratio grows. Since in this case  $P_A CO_2$  does not move from its controlled value of 40 mmHg, most of the increase of the  $\frac{\dot{V}_A}{\dot{Q}}$  ratio, apart from the changes of  $RQ_M$  due to the progressively greater fraction of aerobic energy derived from glycogen oxidation (see Chap. 1), is due to the widening of  $(CaO_2 - C\bar{v}O_2)$ . However, as long as we operate on the flat part of the oxygen equilibrium curve,  $CaO_2$  does not vary, so that an increase of  $(CaO_2 - C\bar{v}O_2)$  can be sustained only by a fall of  $C\bar{v}O_2$ . This is inevitably associated with an increase in  $C\bar{v}CO_2$ , so it moves the mixed venous point of an  $O_2$ – $CO_2$  diagram upwards and leftwards. Since the inspired air point is unchanged as long as we breathe air at sea level, the shape of the ideal air curve is modified at exercise with respect to rest, as represented in Fig. 2.7.

The direct proportionality between  $\dot{V}_A$  and  $-\dot{V} CO_2$  implies invariance of their ratio, and thus of  $P_A CO_2$ . The tight matching between  $\dot{V}_A$  and  $-\dot{V} CO_2$  is the result of a fine regulation, mostly centred on the activity of the central chemoreceptors and the characteristics of their response. This equilibrium is broken in case of

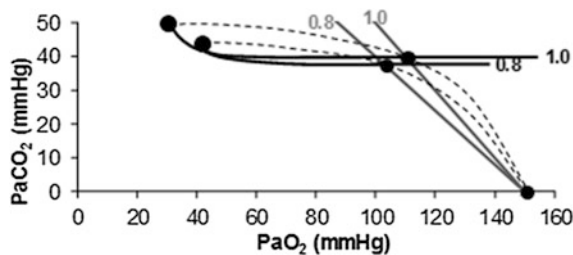


**Fig. 2.7** Displacement of ideal air curve at exercise with respect to rest. The changes in the partial pressures of respiratory gases at exercise move the mixed venous point upwards and leftwards, without changes in inspired air composition. The ideal air curve is modified accordingly. Note that the ideal alveolar air composition is affected also by the change of the metabolic respiratory quotient during exercise

hyperventilation, when  $\dot{V}_A$  increases in the absence of a proportional increase of metabolism, i.e. of  $-\dot{V}\text{CO}_2$ , so that their ratio goes up: in this case, the new steady state is attained at a lower value of  $P_A\text{CO}_2$ . This is so, e.g. at high altitude, due to hypoxic stimulation of peripheral chemoreceptors, or in case of pathological disturbances of  $\frac{\dot{V}_A}{Q}$  ratio heterogeneity in the lungs. The reverse takes place when hypoventilation occurs, as in case of respiratory failure or of paralysis of the respiratory centres.

Equilibration between alveolar air and arterial blood is the main assumption behind the ideal air curve. This equilibration in normoxia occurs indeed in each pulmonary capillary which is in contact with an alveolus, provided the contact time between alveolar air and capillary blood is long enough. According to Wagner and West (1972), at rest, full equilibration between the two sides of the alveolar–capillary barrier is attained when the blood has completed about one-third of the capillary length, this fraction increasing at exercise due to higher blood flow. In spite of this,  $P_a\text{O}_2$  is lower than  $P_A\text{O}_2$  in real lungs. This is a consequence of the combined effect of the heterogeneity of  $\frac{\dot{V}_A}{Q}$  distribution in the lungs and of the shape of the oxygen equilibrium curve. Alveoli perfused by capillaries in a lung segment with elevated  $\frac{\dot{V}_A}{Q}$  ratio are characterized by high  $P_A\text{O}_2$  and end-capillary  $PO_2$  values, in perfect equilibrium; on the other side, alveoli perfused by capillaries in a lung segment with low  $\frac{\dot{V}_A}{Q}$  ratio are characterized by low  $P_A\text{O}_2$  and end-capillary  $PO_2$  values, again in perfect equilibrium. One would expect that the former capillaries would compensate for the latter capillaries, when capillary blood is mixed to form arterial blood in the pulmonary vein, pretty much as air coming from different alveoli does in the trachea, where it forms the mean alveolar air that is analysed at the end of a prolonged expiration. This averaging of blood coming from different capillaries occurs indeed; however, in contrast with alveolar air, it is the binding of oxygen to haemoglobin with allosteric kinetics that dictates blood oxygen concentration at any  $PO_2$ , through an oxygen equilibrium curve that is sigmoidal. On one side, the blood draining from capillaries with low  $\frac{\dot{V}_A}{Q}$  ratio has a decreased end-capillary  $PO_2$ , close to the steep part of the oxygen equilibrium curve, so that their oxygen concentration is reduced indeed. On the other side, the blood draining from capillaries with high  $\frac{\dot{V}_A}{Q}$  ratio has an increased end-capillary  $PO_2$ , located on the flat part of the oxygen equilibrium curve, so that their oxygen concentration is not or minimally increased, which prevents them from compensating for the effect of the capillaries with low  $\frac{\dot{V}_A}{Q}$  ratio. This is the cause of the reduction of  $P_a\text{O}_2$  with respect to  $P_A\text{O}_2$  and of the appearance of the **alveolar–arterial pressure difference**. This state of things is illustrated in Fig. 2.8. The same is not the case for carbon dioxide, because of the steepness of a linear carbon dioxide equilibrium curve in the physiological range.

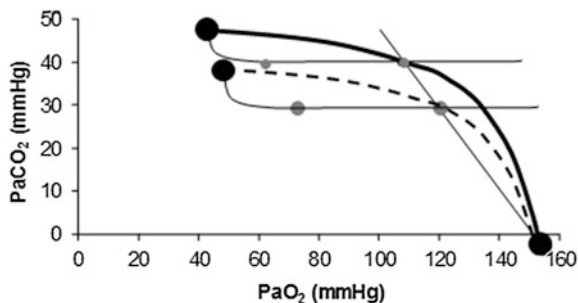


**Fig. 2.8** Identification of the alveolar–arterial oxygen pressure difference on the  $O_2$ – $CO_2$  diagram as the horizontal distance between the two grey dots on a given respiratory quotient isopleth for blood. The effects of hyperventilation (*dashed curve*) are also shown. Note that hyperventilation does not change the alveolar–arterial oxygen pressure difference

## Diffusion–Perfusion Interaction in Alveolar–Capillary Gas Transfer

Alveolar–capillary gas transfer is the result of two interrelated mechanisms: diffusion across the alveolar–capillary barrier, and lung capillary perfusion. At steady state, the flow of gas (e.g. oxygen) leaving the lungs through capillary blood must be equal to the flow of gas that crosses the alveolar–capillary barrier. This can be described with a very simple model of a meta-capillary with steady blood flow, which is in contact for its entire length with a meta-alveolus through a thin, homogeneous membrane. This is tantamount to imagine the mean pulmonary blood flow in contact with the mean alveolar air, with oxygen diffusing across a mean alveolar–capillary barrier. If this is so, the gas flow  $\dot{V}$  across the membrane of given surface area  $A$  and thickness  $L$  is directly proportional to the pressure gradient across that membrane:

$$\dot{V} = \Delta P \left( \frac{dsA}{L} \right) = \Delta P D_L \quad (2.19)$$

where  $d$  and  $s$  are the diffusion and solubility constants of the gas at stake in the barrier, and  $D_L$  is the lumped constant called **lung diffusing capacity**.  $\Delta P$  is the effective pressure gradient, i.e. the difference between  $P_{AO_2}$  and the pressure existing in the capillary at a given distance  $\delta$  from the venous entrance [ $P_c(\delta)$ ]. For the specific case of oxygen, the diffusive  $\dot{V}_{O_2}$  across the barrier at any distance  $\delta$  is thus equal to

$$d\dot{V}_{O_2} = [P_{AO_2} - P_cO_2(\delta)]D_L \quad (2.20)$$

The infinitesimal  $d\dot{V}O_2$  across the barrier progressively raises the  $P_cO_2$  at  $\delta$  from the venous to the arterial side in inverse proportion to blood flow  $\dot{Q}$  and to the gas transport coefficient in blood (for oxygen,  $\beta_b$ )

$$d\dot{V}O_2 = \dot{Q}\beta_b dP_cO_2 \quad (2.21)$$

For inert gases,  $\beta$  is a constant that is independent of the gas pressure. For oxygen,  $\beta_b$  does depend on  $P_cO_2$ , because of the allosteric characteristics of oxygen binding to haemoglobin. If for simplification we assume  $\beta_b$  invariant, i.e. we take the average slope of the oxygen equilibrium curve as the invariant  $\beta_b$  value, the rate of increase of  $P_cO_2$  along the capillary tends to an asymptote corresponding to  $P_AO_2$  (Krogh 1922). On this basis, at steady state, combination of Eqs. (2.20) and (2.21) and subsequent integration along the capillary length yields

$$\frac{(P_AO_2 - P_c'O_2)}{(P_AO_2 - P_vO_2)} = e^{-\frac{D_L}{\dot{Q}\beta_b}} \quad (2.22)$$

where  $P_c'O_2$  is end-capillary  $PO_2$ . This equation has been defined as the **lung diffusion-perfusion interaction equation**. The left-end branch of Eq. (2.22) was defined as **equilibration deficit**, whose value depends only on the **equilibration coefficient**, i.e. on the exponent of the right-hand branch of the same equation, which is the ratio between the diffusive ( $D_L$ ) and perfusive ( $\dot{Q}\beta$ ) conductances (Piiper and Scheid 1981). When the equilibration coefficient is large ( $>3$ ), the equilibration deficit tends to 0 and the gas flow is limited by perfusion; when the equilibration coefficient is small ( $<0.1$ ), the equilibration deficit tends to 1 and the gas flow is limited by diffusion. For a gas like oxygen, which is mostly carried by haemoglobin, diffusion limitation occurs when we operate on the steep part of the oxygen equilibrium curve (e.g. in deep hypoxia), perfusion limitation when we operate on the flat part of the oxygen equilibrium curve (e.g. in hyperoxia). For all gases which do not bind to haemoglobin, and thus which follow the law of Henry, gas flow is limited by perfusion. The flow of carbon monoxide, which has an extremely high affinity for haemoglobin, is limited by diffusion. Generally speaking, there is diffusion limitation whenever  $\beta$  has a high value; conversely, when  $\beta$  tends to 0, there is perfusion limitation. Differences in equilibration coefficient among various gases do not depend on the geometric factors (surface area and thickness of the barrier), which in a given individual are the same for all gases. They depend only on  $d$  and  $s$ , which are included in  $D_L$ , and on  $\beta$ , so that the equilibration coefficient of each gas is proportional to the ratio  $ds/\beta$ . Thus, for any given  $\dot{Q}$  value, the ratio between the equilibration coefficients of two gases is equal to the ratio between the respective  $ds/\beta$ .

A key aspect of the diffusion-perfusion interaction equation is the role played by the contact time ( $t_c$ ), which is the time taken by a given amount of blood to move along capillary and which corresponds to the ratio of the effective lung capillary



blood volume ( $q_c$ ) to  $\dot{Q}$ . On this basis, the equilibration coefficient ( $K_e$ ) can be expressed as follows:

$$K_e = -\frac{D_L t_c}{q_c \beta_b} \quad (2.23)$$

At rest,  $q_c$  is essentially invariant and independent of  $\dot{Q}$ . It increases at exercise, due to the recruitment of previously closed capillaries. For any given  $q_c$  value,  $t_c$  is shorter, the higher is  $\dot{Q}$ . This combination lowers  $K_e$  at exercise, thus increasing the equilibration deficit, and opening the way towards diffusion limitation.

## Breathing Pure Oxygen and the Correction for Nitrogen

Breathing in air concerns three main gases, two of which participate in metabolism and gas exchange, while the third, nitrogen, is inert. Conversely, when breathing pure oxygen, after nitrogen has been completely washed out, only metabolic gases are involved in respiration. In this condition,  $RQ_L$  is necessarily equal to  $-1$ , independent of the cell  $RQ_M$ , so that inspired and expired ventilations are equivalent. This is so because pressure equilibration for differences between  $\dot{V}O_2$  and  $\dot{V}CO_2$  is due to the displacement of an equivalent mass of oxygen instead of nitrogen. Under these conditions,

$$P_A CO_2 = P_I O_2 - P_A O_2 \quad (2.24)$$

On the  $O_2$ – $CO_2$  diagram, this implies that the families of  $RQ_L$  isopleths, that we have when we breathe air, reduce to the one and only possible isopleth for  $RQ_L = -1$ , which at sea level intercepts the  $x$ -axis at  $P_A O_2 = P_I O_2 = 713$  mmHg, i.e. at a value corresponding to the barometric pressure of dry air. This situation is represented on an  $O_2$ – $CO_2$  diagram in Fig. 2.9. On the same figure, we find also two  $RQ_L$  isopleths for a man who breathes air at sea level, namely those for  $RQ_L = -0.8$  and  $RQ_L = -1$ , with the corresponding alveolar gas composition.

The  $O_2$ – $CO_2$  diagram of Fig. 2.9 allows calculation of  $P_I N_2$  and  $P_A N_2$  during air breathing.  $P_I N_2$  is equal to the difference between the barometric pressure of dry air and  $P_I O_2$ , which in Fig. 2.9 corresponds to the horizontal distance, along the  $x$ -axis, between the inspired air compositions during oxygen breathing and during air breathing. Similarly,  $P_A N_2$  during air breathing is equal to the horizontal distance between the alveolar air compositions during oxygen and air breathing, for  $P_A CO_2 = 40$  mmHg. When  $RQ_L = -1$ , the  $RQ_L$  isopleths for oxygen and air breathing are parallel and  $P_A N_2 = P_I N_2$ ; when  $RQ_L > -1$ , the  $RQ_L$  isopleths for oxygen and air breathing diverge and  $P_A N_2 > P_I N_2$ , thus allowing pressure equilibration when  $\dot{V}CO_2 < \dot{V}O_2$ , as much as predicted by Eq. (2.9).

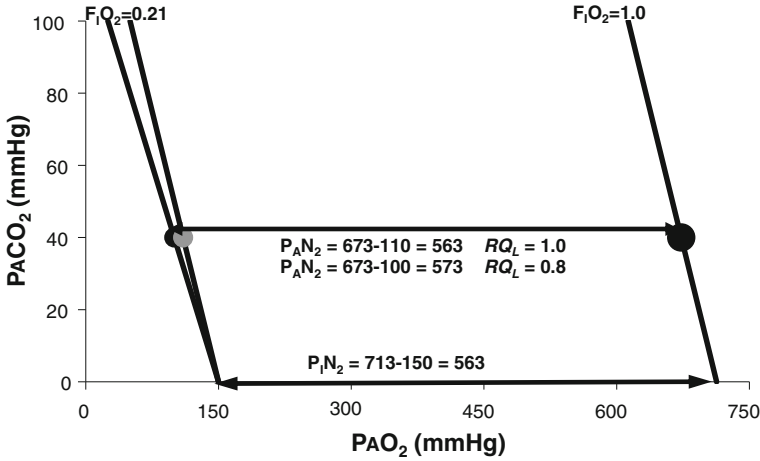


**Fig. 2.9** The effects of breathing pure oxygen on alveolar gas composition. *Horizontal arrows* indicate the inspired and alveolar nitrogen partial pressures. Note that the latter varies when the lung respiratory quotient during air breathing is increased from  $-0.8$  (black dot) to  $-1.0$  (grey dot).  $P_I N_2$ , nitrogen partial pressure in inspired air;  $P_A N_2$ , nitrogen partial pressure in alveolar air;  $R_{Q_L}$ , lung respiratory quotient;  $F_I O_2$ , inspired oxygen fraction

## The Mechanical Efficiency of Exercise

When animals move, they perform mechanical work, i.e. they displace their body mass from a site to another covering the distance (length) between the two sites. The shorter is the time that is necessary to cover a given distance, the greater is the power (work per unit of time) that they have to develop. To do this, animals rely on muscular contraction. Muscles are biological engines, which transform the chemical energy liberated by biological substrates (mostly lipids and glycogen) in oxidative processes in mechanical work. The **mechanical efficiency** ( $\eta$ ) of this energy transformation is given by

$$\eta = \frac{W}{E} \quad (2.25)$$

Normally, the amount of work performed is less than the chemical energy transformed, so that  $\eta < 1$ . During contractions implying muscle shortening—concentric contractions— $\eta = 0.25$ . This means that, of the overall amount of chemical energy transformed, a quarter becomes mechanical work: the remainder is lost as heat. The rate, at which chemical energy is transformed into mechanical work and heat during exercise, is defined as the **metabolic power** of exercise [term  $\dot{E}$  of Eq. (2.1)]. Of course, the metabolic power is not entirely used for exercise: a resting individual does not perform mechanical work to move his body—does not perform exercise—yet he has a positive metabolic power (resting metabolic power,

$\dot{E}_R$ , some 105 W on average) sustaining resting  $\dot{V}_A$  and  $\dot{Q}$ , smooth muscle contraction and chemicals displacement against concentration gradients, plus the isometric muscle contractions that sustain a standing or sitting body.

As already pointed out, during light dynamic exercise, the general equation of the energetics of muscular exercise reduces to Eq. (2.2). This equation indicates that all energy sustaining the development of mechanical power ( $\dot{w}$ ) during exercise derives from aerobic energy sources, so that a simple measure of  $\dot{V}O_2$  provides a complete and satisfactory measure of  $\dot{E}$ . If  $\eta$  is invariant, then the increase in  $\dot{E}$  above its resting value must be proportional to the increase in  $\dot{w}$ , whence a linear relationship between  $\dot{E}$  and  $\dot{w}$  at exercise. This is indeed what happens during dynamic light exercise on a cycle ergometer, the most common type of exercise in a laboratory of integrative physiology nowadays, as shown in Fig. 2.10. This is not so, however, during walking, in which the relationship between  $\dot{E}$  and  $\dot{w}$  (i.e. speed) is nonlinear, indicating changes of  $\eta$  as a function of speed.

The linear relationship depicted in Fig. 2.10 takes the following algebraic form:

$$\dot{E} = \dot{E}_0 + \zeta \dot{w} \quad (2.26)$$

where the y-intercept  $\dot{E}_0$  should correspond to  $\dot{E}_R$ —in fact  $\dot{E}_0$  is slightly higher than  $\dot{E}_R$ , as we will see. In turn, the angular coefficient  $\zeta$  is equal to

$$\zeta = \frac{d\dot{E}}{d\dot{w}} \quad (2.27)$$

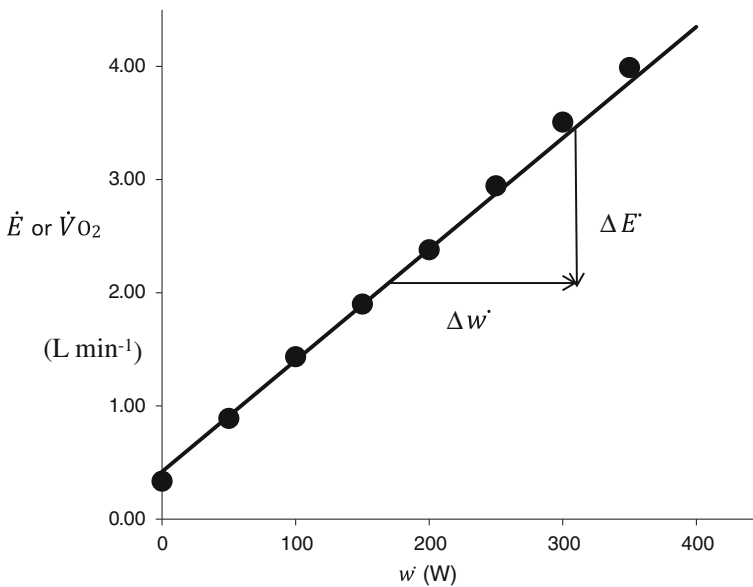


**Fig. 2.10** The dots refer to unpublished data obtained on a top-level cyclist. The slope of the regression line is equal to the reciprocal of the mechanical efficiency of exercise

which, according to Eq. (2.25), is the reciprocal of  $\eta$ , for which a value between 0.23 and 0.25 is in most cases obtained. Thus, Fig. 2.10 tells that, during dynamic light exercise on a cycle ergometer, (i)  $\eta$  is constant indeed, as predicted; (ii) the higher is  $\zeta$  (greater increase in  $\dot{E}$  per unit increase in  $\dot{w}$ ), the lower is  $\eta$ ; and (iii)  $\eta$  corresponds pretty well to the mechanical efficiency of concentric muscle contractions (Gaesser and Brooks 1975). When  $\eta$  is calculated after Eq. (2.26), as the reciprocal of  $\zeta$ , it is sometimes called the **delta-efficiency** of exercise.

The net rate of metabolic energy expenditure ( $\dot{E} - \dot{E}_R$ , where  $\dot{E}_R < \dot{E}_0$ ) is equal to the sum of the rates of energy expenditure required to overcome external ( $\dot{E}_E$ ) and internal ( $\dot{E}_I$ ) powers. On the one side,  $\dot{E}_E$  is the metabolic power actually used to overcome  $\dot{w}$ , whence  $\dot{E}_E = \dot{E} - \dot{E}_0$ ; on the other side,  $\dot{E}_I$  is dissipated against all other resistances than that imposed by  $\dot{w}$ , so that  $\dot{E}_0 = \dot{E}_R + \dot{E}_I$ , which explains why  $\dot{E}_0 > \dot{E}_R$ , as pointed out above. On this basis, Eq. (2.26) can be rewritten as follows:

$$\dot{E} - \dot{E}_R = \dot{E}_{NET} = \dot{E}_I + \dot{E}_E = \dot{E}_I + \zeta \dot{w} \quad (2.28)$$

According to this equation,  $\dot{E}_I$  is independent of  $\dot{w}$ . It was also demonstrated that  $\dot{E}_I$  is a power function of the pedalling frequency ( $f_p$ ) (Francescato et al. 1995) and is a linear function of the weight of the legs, that is the product of the mass of the legs ( $ML$ ) times the gravity acceleration ( $a_g$ ) (Girardis et al. 1999).

$$\dot{E}_I = \varepsilon ML a_g \quad (2.29)$$

where the constant  $\varepsilon$ , which has the dimension of a velocity, contains the length of the pedal lever and  $f_p$ . Bonjour et al. (2010) demonstrated that  $\varepsilon$  varies with the square of  $f_p$ , so that we can write

$$\dot{E}_I = \phi f_p^2 ML a_g \quad (2.30)$$

Bonjour et al. (2010) obtained for the proportionality constant  $\phi$  a value of 1.73 m s.

Studies during walking and running demonstrated that in both cases  $\eta$  is higher than 0.25. During walking, this is due to the fact that, since kinetic and potential energy are in opposition of phase, horizontal speed is largely sustained by continuous exchanges between these two forms of energy with an efficiency of 1, as in a pendulum. In running, the elastic strain energy that is absorbed by the tendons whenever a foot touches the ground and brakes the fall of the body is immediately returned in the subsequent bounce, again with an efficiency of 1 (Cavagna and Kaneko 1977; Cavagna et al. 1976). During uphill walking and running, at least at slopes above 20 %, all energy is expended to lift the body: the former two mechanisms are not functional anymore, and only concentric muscle contractions are carried out, with  $\eta$  equal to 0.25; conversely, during downhill walking and running, at least at negative slopes below -20 %, all energy is expended to brake the body fall: only eccentric muscle contractions occur, with  $\eta$  equal to 1.20 (Minetti et al. 2002).

## Energy Cost of Locomotion

During exercise on a cycle ergometer, the pedalling individual does not move forward on a horizontal plane. The metabolic power is used to generate pedal rotational speed and overcome the resistance opposed by the brake applied on the cycle ergometer. In actual locomotion, the body does move forward in a given direction on the horizontal plane at given speeds ( $v_h$ ). At steady state, the mean  $v_h$  does not vary with time. Of course,  $\dot{E}$  and  $\dot{w}$  increase with  $v_h$ . The slope of a relationship between  $\dot{E}$  and  $v_h$  has the dimension of a force, and it represents the amount of metabolic energy that a moving animal must expend to cover a unit of distance: it is called the **energy cost** ( $C$ ), so we can write

$$C = \frac{\dot{E}}{v_h} \quad (2.31)$$

The relationship between  $\dot{E}$  and  $v_h$  is nonlinear for any type of locomotion: its slope gets higher the higher is  $v_h$ , implying that  $C$  increases with  $v_h$ . A positive  $C$  is needed to overcome the forces that oppose to the horizontal movement of the body. These forces are of two types: frictional forces ( $F_f$ ) and aerodynamic forces—air resistance or drag ( $D$ ), see e.g. di Prampero (1986). Since  $C$  includes metabolic, not mechanical, energy, we can thus write

$$C \eta = F_f + D \quad (2.32)$$

$D$  is proportional to the square of speed:

$$D = k_d v_h^2 \quad (2.33)$$

where constant  $k_d$  is proportional to air density ( $\rho$ ), the drag coefficient ( $C_x$ ), and the projection area on the frontal plane ( $A$ ):

$$k_d = 1/2 \rho C_x A \quad (2.34)$$

$\rho$  is some 800 times greater for water than for air, whence the much higher  $C$  in swimming than in any type of locomotion on land. In air,  $\rho$  is directly proportional to  $P_B$  and inversely proportional to temperature.  $C_x$  is a non-dimensional number depending on the surface characteristics, on the geometrical shape of the moving body, and on the characteristics of the air flow around the moving body. A corresponds to the surface area of the body that faces air on the direction of movement. If we introduce Eq. (2.34) into Eq. (2.33), and we divide by  $A$ , we obtain

$$DA^{-1} = 1/2 \rho C_x v_h^2 = P_D \quad (2.35)$$



**Fig. 2.11** A picture of Chris Boardman on his aerodynamic bicycle during his successful 1-h world record attempt at Manchester, UK, on 6 September 1996

where  $P_D$  is the dynamic pressure exerted on the moving body. *Ceteris paribus*,  $P_D$  is directly proportional to  $C_x$ , so that dynamically favourable shapes are characterized by low  $C_x$  values, as is the case for aerodynamic contemporary cars or track bicycles used for record trials (Capelli et al. 1993; di Prampero 2000) (see Fig. 2.11)

Since  $D$  is a force, in analogy with  $C$ , it can be expressed as mechanical work per unit of distance (Ferretti et al. 2011), so that

$$D = C_D \eta = k_d v_h^2 \quad (2.36)$$

where  $C_d$  is the fraction of  $C$  that overcomes  $D$ . As a consequence,

$$C_D = k_d \eta^{-1} v_h^2 = k' v_h^2 \quad (2.37)$$

We can also define the metabolic power against air resistance ( $\dot{E}_D$ ) as the product of  $C_d$  times  $v_h$ . By inserting this definition of  $\dot{E}_D$  into Eq. (2.37), we obtain

$$\dot{E}_D = C_d v_h = k' v_h^3 \quad (2.38)$$

which indicates that  $\dot{E}_D$  is directly proportional to the cube of  $v_h$ .

Let us now consider also the metabolic power against frictional forces ( $\dot{E}_f$ ), which corresponds to the remainder fraction of the net rate of energy expenditure  $\dot{E}_n$ . We then have

$$\dot{E}_n = \dot{E}_D + \dot{E}_f = k'v_h^3 + \dot{E}_f \quad (2.39)$$

A comprehensive analysis of the relationships between  $\dot{E}_n$  and  $v_h$  in several types of locomotion on flat terrain in air at sea level is presented in Fig. 2.12 (di Prampero 1986; Ferretti et al. 2011). In Fig. 2.12, the bold curve is theoretical and applies for  $\dot{E}_n = \dot{E}_D$  ( $\dot{E}_f = 0$  W). Its slope corresponds to  $C_D$ . It is constructed for a  $k'$  value of  $0.774 \text{ J s}^2 \text{ m}^{-3}$  (di Prampero 1985). Note that the curve is flatter and thus apparently displaced rightwards and downwards, the lower is  $k'$ , as when riding aerodynamic bicycles (Capelli et al. 1993), or when cycling at altitude (di Prampero 2000); it becomes steeper when  $k'$  is increased, as when riding ancient bicycles (Minetti et al. 2001). It represents a limit that cannot be overcome on its right side. All other curves in Fig. 2.12 appear leftwards with respect to the bold curve, because of  $\dot{E}_f$ , whose value is higher, the more the experimental curve appears to the left of the bold curve. The vertical distance between each experimental curve and the

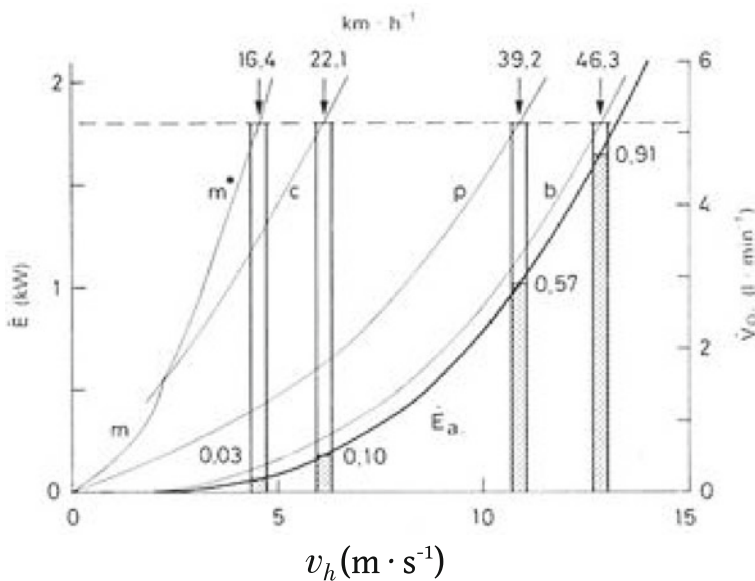


**Fig. 2.12** Metabolic power ( $\dot{E}$ , left ordinate) or oxygen uptake ( $\dot{V}O_2$ , right ordinate) as a function of forward speed ( $v_h$ ). The bold curve refers to locomotion in which only work against air resistance is carried out. These curves refer to actual locomotion ( $b$ , bicycling;  $p$ , skating;  $c$ , running;  $m$ , walking;  $m^*$ , competitive walking). Histograms indicate the fraction of metabolic power expended against aerodynamic forces. The speed on top of each histogram is the maximal aerobic speed for an athlete with a maximal oxygen consumption of  $5 \text{ L min}^{-1}$ . After di Prampero (1985)

**Table 2.1** Parameters describing various types of human locomotion on land. Data taken from Ferretti et al. (2011)

Locomotion mode	$k'(\text{J s}^2 \text{ m}^{-3})$	$C_x$	$C_f(\text{J m}^{-1} \text{ kg}^{-1})$
Running	0.72	1.10	3.9*
Skating	0.79	0.50	1.0
Cycling, race	0.77	0.75	0.17
Cycling, traditional	1.14	1.00	0.27
Cycling, aerodynamics	0.58	0.65	0.15

\*indicates an average value: in fact  $C_f$  varies linearly with the running speed

theoretical curve corresponds to  $\dot{E}_f$ .  $\dot{E}_f$  is directly proportional to  $v_h$ . Thus, the energy cost against frictional forces ( $C_f$ ) is a constant that is independent of  $v_h$ . In fact  $C_f$  corresponds to the  $y$ -intercept of the linear relationship between  $C$  and  $v_h^2$ , with slope equal to  $k'$ , since

$$C = C_D + C_f = k' v_h^2 + C_f \quad (2.40)$$

$C_f$  depends on the characteristics of the interaction between the terrain and the foot or the device (wheel, skates, skis). In cycling, it depends on the width and type of the tyres, on their filling pressure and on the characteristics of the terrain. It is also proportional to the overall weight of bicycle plus human (di Prampero 2000). Average values for  $k'$ ,  $C_x$  and  $C_f$  are reported in Table 2.1 for different types of locomotion.

Some practical consequences of Fig. 2.12 and Table 2.1 are (i) the fraction of  $C$  represented by  $C_d$  and  $C_f$  varies with the locomotion mode; (ii)  $k'$  is remarkably similar among different locomotion modes; (iii)  $\dot{E}_D$  at any given is similar among locomotion modes—except walking; and (iv) differences in  $v_h$  among various locomotion modes are essentially due to differences in  $\dot{E}_f$ . Particularly in cycling,  $\dot{E}_f$  is minimized by the rotational movement of the wheel, by the amplification effect of the gear and by the absence of work against gravity due to body stabilization by the bike, so that most of  $\dot{E}$  can indeed be used to overcome air resistance. This is why cycling leads to reach the highest speeds in human locomotion.

Walking takes place in a speed range where  $C_d$  is negligible, so that, practically speaking,  $\dot{E} = \dot{E}_f$ . But walking, with respect to all other types of locomotion, is peculiar, because of the effects of pendulum-like mechanism and the ensuing transformation of potential energy into kinetic energy and vice versa. Concerning running,  $C$  was generally considered invariant in a given individual and thus independent of the running speed (di Prampero 1986; Ferretti et al. 2011), possibly as a consequence of the fact that most data were obtained during treadmill running, a condition in which the running human moves with respect to the treadmill's belt, but not with respect to air (Dill 1965; di Prampero et al. 1986; Hagberg and Coyle 1984; Helgerud 1994; Margaria et al. 1963; McMiken and Daniels 1976; Minetti et al. 2002; Padilla et al. 1992, to give a few examples). Yet Pugh (1970)



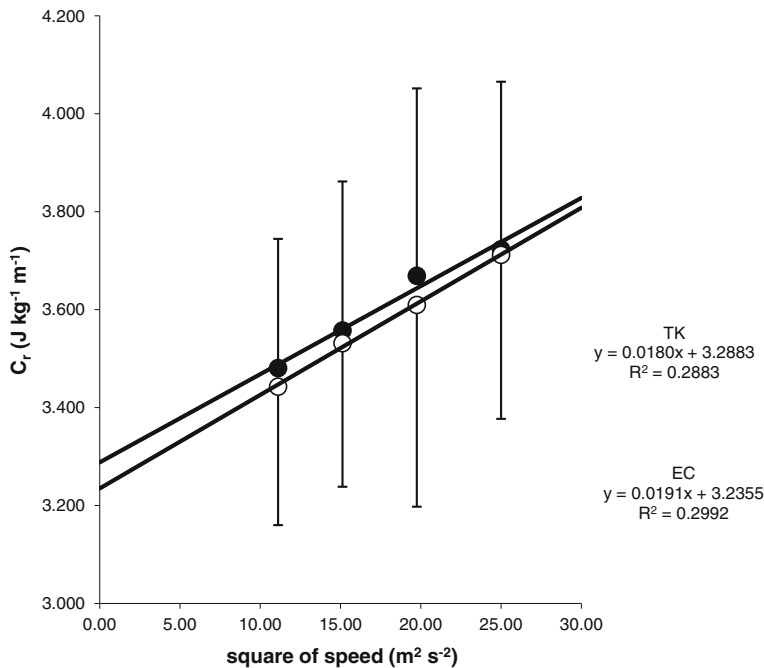


**Fig. 2.13** Energy cost of running ( $C_r$ ) as a function of the square of speed in top-level marathon runners from Kenya (black dots) and from Europe (white dots). From Tam et al. (2012)

demonstrated that a fraction of  $C$  varies with the square of wind velocity, although this fraction was considered small. Following his study, the concept that  $C$  could be slightly higher during track than during treadmill running, although still independent of speed, started to be admitted (di Prampero 1986; Jones and Doust 1996; Léger and Mercier 1984). I believe that the reason why it was hard to identify a clear effect of air resistance on  $C$  during running is related to the relatively low running speeds tested in most studies. In fact, the first demonstration that Eq. (2.40) applies also to running was obtained by Tam et al. (2012) on top-level marathon runners from Kenya, who were able to run in submaximal condition at speeds up to  $20 \text{ km h}^{-1}$  (Fig. 2.13); and that it was a clear effect of  $C_d$  is also demonstrated by the results of Helgerud et al. (2010), who found no differences in  $C$  as a function of  $v_h$  during treadmill running at similar speeds to those of Tam et al. (2012).

$C$  is related also to the technical ability of the individual in a given locomotion mode: in general, the better is the technique of movement, the lower is  $C$ , so that, because of Eq. (2.31), at any given  $\dot{E}$  value higher  $v_h$  can be attained. This has little importance in running, in which, although top-level runners have lower  $C$  than leisure runners or non-habitual runners (di Prampero 1986), little changes in  $C$  can be obtained with training (Morgan et al. 1989). On the contrary, in swimming, impressive decreases of  $C$  can be achieved by improving the swimming technique (Holmér 1974). Termin and Pendergast (2000) demonstrated that continuous swimming training on multiple

year basis reduces  $\dot{E}$  and the stroke frequency ( $f_s$ ) at any speed, thus increasing the distance covered by a stroke, with consequent drop of  $C$ . Swimming, although it follows the general rules described by Eqs. (2.31) and (2.36), is nevertheless characterized by some peculiarities related to the fact that it takes place in water, whose  $\rho$  is some 800 times greater than that of air, so that (i) buoyancy counts much more than gravity acceleration; (ii) for a given  $\dot{E}$ ,  $C$  is much higher and  $v_h$  much lower than in any other type of locomotion on land; (iii) due to differences in buoyancy between the upper and the lower part of the body, torque tends to increase  $A$ , and thus  $k_d$  and  $C$  (Pendergast et al. 1977; Zamparo et al. 2009); (iv) due to differences in body composition, torque is less in women than in men, whence a lower  $C$  in the former than in the latter (Zamparo et al. 2008) at a given speed; (v) the effects of torque are counteracted by feet movements, so that, although all external power transmits kinetic energy to water, only a fraction of the external power is actually used to propel the body on the horizontal plane (Zamparo et al. 2011); as a consequence, (vi) the overall  $\eta$  of swimming is less than that of concentric muscle contractions (for a detailed discussion of  $\eta$  during swimming, see Zamparo et al. 2002).

## The Cardiovascular Responses to Exercise

The main factor characterizing the cardiovascular responses to exercise is the increase in  $\dot{Q}$ , due to the simultaneous increase of its two determinants, the heart rate ( $f_h$ ) and the stroke volume ( $Q_s$ ) (Asmussen and Nielsen 1952; Åstrand et al. 1964; Hermansen et al. 1970; Stenberg et al. 1967). This increase is classically attributed to a remodulation of autonomic nervous system control of heart activity at exercise (Fagraeus and Linnarsson 1976; Robinson et al. 1966), although the effect of the Frank–Starling mechanism on  $Q_s$  has been considered as well (Rowell et al. 1996). At steady state,  $\dot{Q}$  is a linear function of  $\dot{V}O_2$  (Åstrand et al. 1964; Cerretelli and di Prampero 1987). The relation has a positive y-intercept, implying, as long as the exercise intensity is increased, there is a smaller growth of  $\dot{Q}$  than of  $\dot{V}O_2$ , so that, according to Eq. (2.3), the  $C\alpha O_2 - C\bar{v}O_2$  difference becomes greater. Most of the increase in  $\dot{Q}$  goes into the active muscle mass, so that muscle blood flow increases remarkably, due to the stimulation of  $\beta_2$ -adrenergic receptors, which are found in muscles instead of  $\alpha_1$ -adrenergic receptors, and to the action of local vasodilating mediators (Delp and Laughlin 1998; Delp and O’Leary 2004; Seals and Victor 1991). Muscle vasodilation determines a sudden drop of total peripheral resistance ( $R_p$ ). Finally, systolic arterial pressure increases, whereas diastolic blood pressure, if any, tends to go down (Rowell et al. 1968).

The linear relationship between  $\dot{Q}$  and  $\dot{V}O_2$  is fairly stable. Aerobic training decreases  $f_H$  and increases  $Q_s$ , so that at any given  $\dot{V}O_2$ ,  $\dot{Q}$  remains unchanged (Ekblom et al. 1968; Saltin et al. 1968). The same is the case for athletes, whose maximal oxygen consumption is higher than that of non-athletic individuals: they have the same  $\dot{Q}$  versus  $\dot{V}O_2$  relationship as non-athletes, with lower  $f_H$  and higher

$Q_s$  (Eklblom and Hermansen 1968). The superposition of arm exercise to leg exercise (Bevegård et al. 1966) and the exercise mode (Hermansen et al. 1970) have no effects on the  $\dot{Q}$  versus  $\dot{V}O_2$  relationship. Water immersion and supine posture, in spite of their acute effects on central blood volume with consequent decrease in  $f_H$  and increase in  $Q_s$ , do not alter the  $\dot{Q}$  versus  $\dot{V}O_2$  relationship (Bevegård et al. 1966; Rennie et al. 1971; Sheldahl et al. 1987). Exercise in the heat, whose effects on  $f_H$  and  $Q_s$  are opposite to those of water immersion, implies reduced  $\dot{Q}$  values at any given  $\dot{V}O_2$  only when heat is extreme and the drop of  $R_p$  for simultaneous muscular and cutaneous vasodilation is dramatic (Nadel et al. 1979; Rowell 1974). Only admitted exceptions to an essentially invariant  $\dot{Q}$  versus  $\dot{V}O_2$  relationship were the upwards shift of the  $\dot{Q}$  versus  $\dot{V}O_2$  relationship in acute hypoxia (Hartley et al. 1973; Hughes et al. 1968; Roca et al. 1989; Stenberg et al. 1966) and after moderate CO poisoning (Vogel and Gleser 1972). The concept of an invariant relationship between  $\dot{Q}$  and  $\dot{V}O_2$  was so deeply rooted in exercise physiologists, that those exceptions were explained in terms of an *error signal*, related to reduced  $CaO_2$  influencing the control system of  $\dot{Q}$  (see e.g. Cerretelli and di Prampero 1987).

Acute hypoxia and CO poisoning share a common aspect, that they both lead to a reduction of  $CaO_2$ . Conversely, when  $CaO_2$  is increased, such as upon return to sea level after altitude acclimatization, the  $\dot{Q}$  versus  $\dot{V}O_2$  relationship is shifted downwards (Ferretti et al. 1990). On these bases, these last authors hypothesized that  $\dot{Q}$  varies in inverse proportion with  $CaO_2$  in order to maintain systemic oxygen delivery ( $\dot{Q}aO_2$ ), i.e. the product of  $\dot{Q}$  times  $CaO_2$ , invariant at any given  $\dot{V}O_2$ . This being the case,  $\dot{Q}aO_2$  rather than  $\dot{Q}$  would be the regulated variable at exercise steady state.

The relationship between  $\dot{Q}aO_2$  and  $\dot{w}$  was investigated by Ferretti et al. (1992) in the  $\dot{w}$  range that allows attainment of a steady state for  $\dot{V}O_2$  at exercise and was found to be linear and parallel to that between  $\dot{V}O_2$  and power. This implies that the vertical difference between the two lines, corresponding to the oxygen flow in mixed venous blood ( $\dot{Q}\bar{v}O_2$ ), is a constant, independent of  $\dot{Q}$  and  $\dot{V}O_2$ , and thus of the exercise intensity. Later,  $\dot{Q}\bar{v}O_2$  was found to depend  $SaO_2$  (Anchisi et al. 2001) and on the activation state of the autonomic nervous system (Ferretti et al. 2005).

## The $\dot{Q} - \dot{V}O_2$ Diagram

On the basis of what precedes, the relationship between  $\dot{Q}$  and  $\dot{V}O_2$  can be analysed under a different perspective. Since, according to Ferretti et al. (1992),  $\dot{Q}\bar{v}O_2$  is equal to

$$\dot{Q}\bar{v}O_2 = K = \dot{Q}aO_2 - \dot{V}O_2 \quad (2.41)$$

If we consider that  $\dot{Q} aO_2$  is the product of  $\dot{Q}$  times  $CaO_2$ , Eq. (2.36) can be rewritten as follows:

$$\dot{Q} \bar{v}O_2 = \dot{Q} \cdot CaO_2 - \dot{V}O_2 \quad (2.42)$$

whose solution for  $\dot{Q}$  is

$$\dot{Q} = \frac{\dot{V}O_2 + \dot{Q} \bar{v}O_2}{CaO_2} \quad (2.43)$$

Cerretelli and di Prampero (1987), in agreement with previous authors who considered  $\dot{V}O_2$  to be set only by  $\dot{w}$ , represented  $\dot{Q}$  as the dependent variable and  $\dot{V}O_2$  as the independent variable. If this is so, Eq. (2.43) tells that  $\dot{Q}$  is linearly related to  $\dot{V}O_2$ , with slope equal to  $CaO_2^{-1}$  and intercept on the  $x$ -axis equal to  $-\dot{Q} \bar{v}O_2$ . Such a relationship is constructed in Fig. 2.14a, where a family of  $CaO_2$  isopleths is reported, all converging on the same  $\dot{Q} \bar{v}O_2$  value, and validated using data obtained in normoxia, taken from different sources in the literature (Adami et al. 2014) (Fig. 2.14b), from which a mean  $\dot{Q} \bar{v}O_2$  value of  $1.35 \text{ L min}^{-1}$  was computed, whereas  $CaO_2^{-1}$  (slope of the  $\dot{Q}$  versus  $\dot{V}O_2$  line) resulted equal to  $4.93 \text{ L of blood per L of oxygen}$ , yielding a theoretical  $CaO_2$  of  $203 \text{ ml L}^{-1}$ . All the data shown in Fig. 2.14b are exercise data, a condition in which the parasympathetic branch of the autonomic nervous system is inactive (Fagraeus and Linnarsson 1976). At rest, in which there is predominant vagal control of heart rate (Fagraeus and Linnarsson 1976; Lador et al. 2006; Malliani et al. 1991; Perini and Veicsteinas 2003), the data lie below those obtained at exercise, compatibly with a lower  $\dot{Q} \bar{v}O_2$  value. This agrees with previous observations, both during cycling (Anchisi et al. 2001; Ferretti et al. 2005) and during two-legged knee extension exercise (Koskolou et al. 1997; Roach et al. 1999). In Fig. 2.14, this implies a right shift of the  $CaO_2$  isopleths.

The very strong dependence of  $\dot{Q}$  on  $\dot{V}O_2$  shown in Fig. 2.14 allows an overall theoretical view of the steady-state cardiovascular responses to exercise as a function of exercise intensity and  $CaO_2$ , based on Fig. 2.14a, which Adami et al. (2014) called **the  $\dot{Q} - \dot{V}O_2$  diagram**. This figure is conceptually different from the classical  $\dot{Q}$  versus  $\dot{V}O_2$  relationship. The latter figure in fact, as  $\dot{V}O_2$  is increased, shows a progressive shift of the  $\dot{Q}$  values towards isopleths for higher arterial–venous oxygen difference, which converge on the origin of the axes (Cerretelli and di Prampero 1987). Conversely the  $\dot{Q} - \dot{V}O_2$  diagram reports  $CaO_2$  isopleths converging on a specific, negative  $x$ -axis intercept, corresponding to  $\dot{Q} \bar{v}O_2$  ( $1.35 \text{ L min}^{-1}$ , according to the regression line of Fig. 2.14b). During moderate exercise in normoxia, the regression line of Fig. 2.14b coincides with a specific  $CaO_2$  isopleth because  $CaO_2$  is fairly invariant. Anaemic individuals (Roach et al. 1999; Woodson et al. 1978), whose  $CaO_2$  is reduced because of [Hb] loss in the

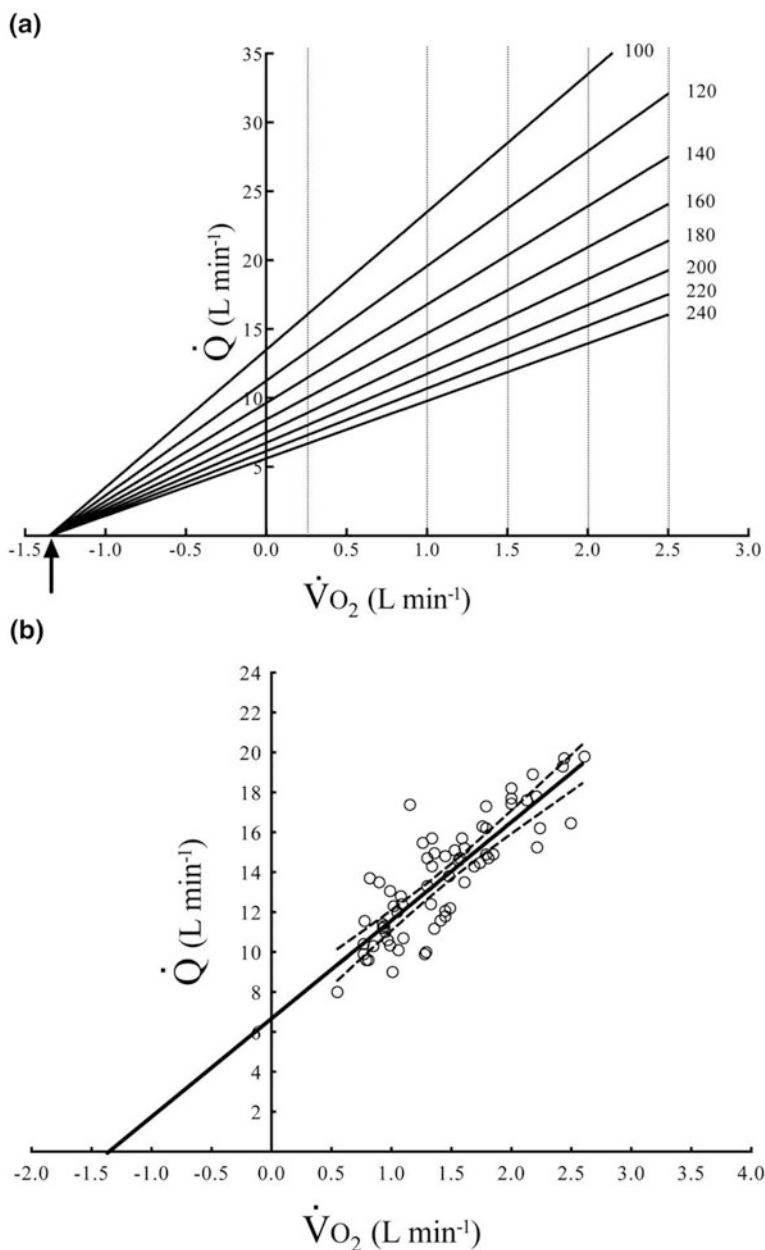


**Fig. 2.14** Panel a Theoretical representation of the relationship between cardiac output ( $\dot{Q}$ ) and oxygen uptake ( $\dot{V}O_2$ ) at exercise steady state ( $\dot{Q} - \dot{V}O_2$  diagram). The lines are isopleths for the indicated values of arterial oxygen concentration. They all converge on the same x-axis intercept, corresponding to the oxygen flow in mixed venous blood. Panel b An experimental  $\dot{Q} - \dot{V}O_2$  diagram obtained during steady-state exercise in normoxia, using data from different sources in the literature. After Adami et al. (2014)

absence of  $SaO_2$  changes, and thus who still operate on the flat part of the oxygen equilibrium curve, would have a  $\dot{Q}$  versus  $\dot{V}O_2$  relationship that coincides with a steeper  $CaO_2$  isopleth on the  $\dot{Q} - \dot{V}O_2$  diagram. The same would be the case in the presence of carbon monoxide poisoning (Gonzalez-Alonso et al. 2001; Vogel and Gleser 1972). On the opposite side, in case of polycythaemia, the  $\dot{Q}$  versus  $\dot{V}O_2$  relationship would coincide with a flatter  $CaO_2$  isopleth. (Celsing et al. 1986; Ekblom et al. 1976; Ferretti et al. 1990, 1992).

Things are different in acute hypoxia, as shown in Fig. 2.15 which reports data obtained at an inspired oxygen fraction of 0.11. The regression analysis indicates  $\dot{Q}\bar{v}O_2 = 1.12 \text{ L min}^{-1}$  and  $CaO_2^{-1} = 6.73 \text{ L of blood per L of oxygen}$ , corresponding to a mean theoretical  $CaO_2$  of  $148.6 \text{ ml L}^{-1}$ . However, at that level of hypoxia, subjects operate on the steep part of the oxygen equilibrium curve, so that any increase in  $\dot{V}O_2$ , and thus in  $\dot{Q}$ , carries along a shortening of capillary blood transit time, resulting in progressively lower  $SaO_2$  values at the arterial end of lung capillaries, so that there are lower  $CaO_2$  values in hypoxia the higher are  $\dot{V}O_2$  and  $\dot{Q}$ . At any given hypoxic inspired oxygen fraction, the progressive  $SaO_2$  reduction shifts the  $\dot{Q}$  versus  $\dot{V}O_2$  data towards an isopleth for lower  $CaO_2$  values, so that (i) the apparent  $\dot{Q}$  versus  $\dot{V}O_2$  line has a higher slope than that for normoxia; and (ii) the same line points towards a higher  $x$ -axis intercept, indicative of an apparently lower  $\dot{Q}\bar{v}O_2$  value (Adami et al. 2014). Anchisi et al. (2001) found lower  $\dot{Q}\bar{v}O_2$  the

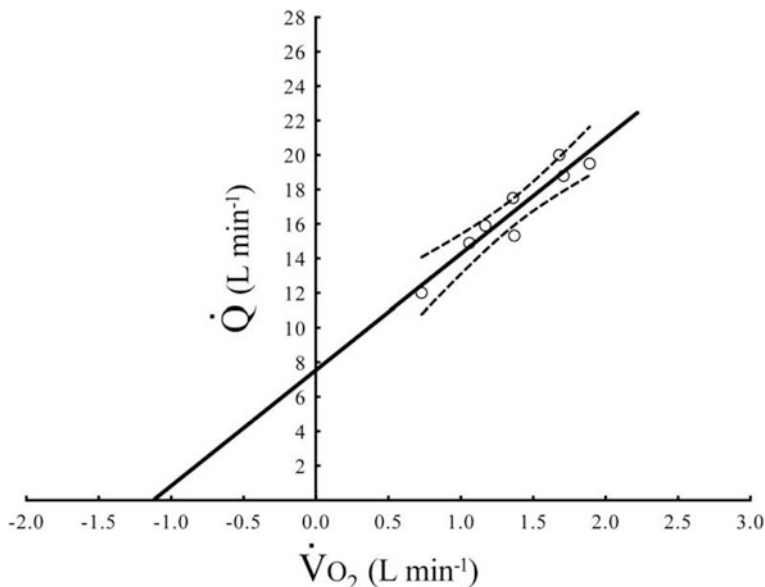


**Fig. 2.15** An experimental  $\dot{Q} - \dot{V}O_2$  diagram constructed for steady-state exercise in acute normobaric hypoxia, using data from different sources in the literature, all obtained at an inspired oxygen fraction of 0.11. After Adami et al. (2014)

lower was the  $SaO_2$ , as discussed here above, but they also found a positive linear relationship between these two parameters at exercise. This means that there is more than a mere shift across  $CaO_2$  isopleths when the  $\dot{Q}$  versus  $\dot{V}O_2$  relationship is modified by a fall of  $SaO_2$  in hypoxia. There is also a right displacement of the  $x$ -axis intercept, implying a decrease of  $\dot{Q}\bar{v}O_2$ . This is at variance with what appears when  $CaO_2$  is modified by changing [Hb] (e.g. anaemia or polycythaemia) while keeping  $SaO_2$  unchanged.

To explain the response characteristics revealed by the  $\dot{Q} - \dot{V}O_2$  diagram, we may call upon different mechanisms, depending on whether there is or not a change in  $SaO_2$ . Oxygen-sensing mechanisms may deserve high consideration. For instance, the conformation of the reduced haemoglobin determines the rise of NO in blood with consequent vasodilatation (Stamler et al. 1997). More recently, Crece-lius et al. (2011a, b) proposed a synergistic effect of prostaglandins and NO in peripheral blood flow regulation during hypoxic exercise. Others suggested that in subjects with reduced  $CaO_2$ , peripheral blood flow may be increased by ATP-mediated vasodilatation (Ellsworth et al. 1995; Gonzalez-Alonso et al. 2002; Mortensen et al. 2011). Stickland et al. (2011) suggested a role for carotid chemoreceptors, directly related to variations of  $CaO_2$ . The above mechanisms, however, do not explain the effect of the  $SaO_2$  fall in hypoxia, as pointed out by Stickland et al. (2011) who excluded a role for carotid chemoreceptors in regulating limb blood flow when  $CaO_2$  was reduced because of a fall in  $SaO_2$ .

## Conclusions

In this chapter, I have described the main relationships that at steady state represent the cardiorespiratory responses to exercise, which are tightly coupled with the metabolic responses to exercise, as a consequence of the concept that at steady state, the same  $\dot{V}O_2$  value is attained at all steps along the respiratory system, from ambient air to mitochondria. To end with, I will try a synthesis of the various relationships that I have discussed. To do so, I would start from the  $\dot{Q} - \dot{V}O_2$  diagram, where  $\dot{Q}\bar{v}O_2$  is defined as a constant, i.e. the  $x$ -axis intercept of a  $\dot{Q}$  versus  $\dot{V}O_2$  line. Its algebraic formulation is summarized in Eq. (2.43). At the same time, the solution for  $\dot{Q}$  of the ventilation-perfusion equation [Eq. (2.18)] is

$$\dot{Q} = \frac{\dot{V}_A P_A CO_2}{CgRQ_L(CaO_2 - C\bar{v}O_2)} \quad (2.44)$$

Inserting Eq. (2.43) in Eq. (2.44) yields

$$\frac{\dot{V}O_2 + \dot{Q}\bar{v}O_2}{CaO_2} = \frac{\dot{V}_A P_A CO_2}{CgRQ_L(CaO_2 - C\bar{v}O_2)} \quad (2.45)$$

Combining also Eq. (2.16) and rearranging, we get

$$\frac{\dot{V}_A P_A CO_2}{CgRQ_L} + \dot{Q}\bar{v}O_2 = \frac{\dot{V}_A P_A CO_2 CaO_2}{CgRQ_L(CaO_2 - C\bar{v}O_2)} = \dot{Q} \cdot CaO_2 \quad (2.46)$$

This equation links ventilation, circulation and metabolism at exercise in a tight manner, such that **homeostasis of the respiratory system at exercise** is maintained around given values of the constant  $\dot{Q}\bar{v}O_2$ . It tells that, as long as we are during steady-state exercise in normoxia, in which  $P_A CO_2$  (40 mmHg) and  $CaO_2$  (200 ml L<sup>-1</sup> for normal haemoglobin concentration) may be considered invariant, any increase in the exercise metabolic rate  $\dot{E}$  and thus in  $\dot{V}O_2$  requires (i) an increase in  $\dot{V}_A$  that is proportional to that in  $\dot{V}O_2$  only if  $RQ_L$  does not change, and (ii) an increase in  $\dot{Q}$  that is not proportional to the corresponding increase in  $\dot{V}O_2$ . Invariance of  $CaO_2$  occurs only as long as we operate on the flat part of the oxygen equilibrium curve (diffusion limitation). As long as diffusion limitation appears, as is the case in deep hypoxia, also  $CaO_2$  varies (drops),  $\dot{Q}$  only partially corrects this drop, the constant  $\dot{Q}\bar{v}O_2$  takes a lower value, and all relations to  $\dot{E}$  are modified except that with  $\dot{V}_A$ , whose characteristics remain related to changes in  $RQ_L$  only: the homeostasis of the respiratory system at exercise is modified. At intense exercise, when lactate accumulation also occurs and hyperventilation superimposes, a new steady state would be attained only at  $P_A CO_2$  values lower than 40 mmHg, depending on the intensity of the hyperventilation: the homeostasis of the respiratory system would again be modified. This new steady state, however, is never attained in fact, and the reasons for this are discussed in Chap. 3. Thus, in real life, the conditions described and discussed in this chapter are observed only during light exercise, below the so-called lactate threshold, or below the called critical power, two concepts that are developed in Chap. 5.

## References

- Adami A, Fagoni N, Ferretti G (2014) The  $\dot{Q} - \dot{V}O_2$  diagram: an analytical interpretation of oxygen transport in arterial blood during exercise in humans. *Respir Physiol Neurobiol* 193: 55–61
- Anchisi S, Moia C, Ferretti G (2001) Oxygen delivery and oxygen return in humans exercising in acute normobaric hypoxia. *Pflügers Arch* 442:443–450
- Armstrong RB, Delp MD, Goljan MF, Laughlin MH (1987) Distribution of blood flow in muscles of miniature swine during exercise. *J Appl Physiol* 62:1285–1298
- Asmussen E, Nielsen M (1952) The cardiac output in rest and work determined simultaneously by the acetylene and the dye injection methods. *Acta Physiol Scand* 27:217–230
- Åstrand PO, Cuddy TE, Saltin B, Stenberg J (1964) Cardiac output during submaximal and maximal work. *J Appl Physiol* 19:258–264



- Baumgartner WA Jr, Jaryszak EM, Peterson AJ, Presson RG, Wagner WW (2003) Heterogeneous capillary recruitment among adjoining alveoli. *J Appl Physiol* 95:469–476
- Bevegård S, Freyschuss U, Strandell T (1966) Circulatory adaptation to arm and leg exercise in supine and sitting position. *J Appl Physiol* 21:37–46
- Bock AV, Vancaulert C, Dill DB, Fölling A, Hurxthal LM (1928) Studies in muscular activity. IV. The steady state and the respiratory quotient during work. *J Physiol* 66:162–174
- Bonjour J, Capelli C, Antonutto G, Calza S, Tam E, Linnarsson D, Ferretti G (2010) Determinants of oxygen consumption during exercise on cycle ergometer: the effects of gravity acceleration. *Respir Physiol Neurobiol* 171:128–134
- Capelli C, Rosa G, Butti F, Ferretti G, Veicsteinas A, di Prampero PE (1993) Energy cost and efficiency of riding aerodynamic bicycles. *Eur J Appl Physiol* 65:144–149
- Cavagna GA, Kaneko M (1977) Mechanical work and efficiency in level walking and running. *J Physiol* 268:467–481
- Cavagna GA, Thys H, Zamboni A (1976) The sources of external work in level walking and running. *J Physiol* 262:639–657
- Celsing F, Nyström J, Pihlstedt P, Werner B, Ekblom B (1986) Effect of long-term anemia and retransfusion on central circulation during exercise. *J Appl Physiol* 61:1358–1362
- Cerretelli P, di Prampero PE (1987) Gas exchange at exercise. In: Farhi LE, Tenney SM (eds) *Handbook of physiology, the respiratory system IV*. Bethesda, MD, pp 555–632 (Am Physiol Soc)
- Clark AR, Tawhai MH, Hoffman EA, Burrows KS (2011) The interdependent contributions of gravitational and structural features to perfusion distribution in a multiscale model of the pulmonary circulation. *J Appl Physiol* 110:943–955
- Cottin F, Médigue C, Papelier Y (2008) Effect of heavy exercise on spectral baroreflex sensitivity, heart rate, and blood pressure variability in well-trained humans. *Am J Physiol Heart Circ Physiol* 295:H1150–H1155
- Crececius AR, Kirby BS, Richards JC, Garcia LJ, Voyles WF, Larson DG, Luckasen GJ, Dinunno FA (2011a) Mechanisms of ATP-mediated vasodilation in humans: modest role for nitric oxide and vasodilating prostaglandins. *Am J Physiol Heart Circ Physiol* 301:H1302–H1310
- Crececius AR, Kirby BS, Voyles WF, Dinunno FA (2011b) Augmented skeletal muscle hyperaemia during hypoxic exercise in humans is blunted by combined inhibition of nitric oxide and vasodilating prostaglandins. *J Physiol* 589:3671–3683
- Delp MD, Laughlin MH (1998) Regulation of skeletal muscle perfusion during exercise. *Acta Physiol Scand* 162:411–419
- Delp MD, O’Leary DS (2004) Integrative control of the skeletal muscle microcirculation in the maintenance of arterial pressure during exercise. *J Appl Physiol* 97:1112–1118
- di Prampero PE (1981) Energetics of muscular exercise. *Rev Physiol Biochem Pharmacol* 89:143–222
- di Prampero PE (1985) *La locomozione umana su terra, in acqua, in aria: fatti e teorie*. Edi Ermes, Milano
- di Prampero PE (1986) The energy cost of human locomotion on land and in water. *Int J Sports Med* 7:55–72
- di Prampero PE (2000) Cycling on earth, in space, on the moon. *Eur J Appl Physiol* 82:345–360
- di Prampero PE, Ferretti G (1999) The energetics of anaerobic muscle metabolism: a reappraisal of older and recent concepts. *Respir Physiol* 118:103–115
- di Prampero PE, Atchou G, Brückner JC, Moia C (1986) The energetics of endurance running. *Eur J Appl Physiol* 55:259–266
- Dill DB (1965) Oxygen used in horizontal and grade walking and running on the treadmill. *J Appl Physiol* 20:19–22
- Ekblom B, Hermansen L (1968) Cardiac output in athletes. *J Appl Physiol* 25:619–625
- Ekblom B, Åstrand PO, Saltin B, Stenberg J, Wallström B (1968) Effect of training on circulatory response to exercise. *J Appl Physiol* 24:518–528
- Ekblom B, Wilson G, Åstrand PO (1976) Central circulation during exercise after venesection and reinfusion of red blood cells. *J Appl Physiol* 40:379–383

- Ellis CG, Wrigley SM, Groom AC (1994) Heterogeneity of red blood cell perfusion in capillary networks supplied by a single arteriole in resting skeletal muscle. *Circ Res* 75:357–368
- Ellsworth ML, Forrester T, Ellis CG, Dietrich HH (1995) The erythrocyte as a regulator of vascular tone. *Am J Physiol Heart Circ Physiol* 269:H2155–H2161
- Fagraeus L, Linnarsson D (1976) Autonomic origin of heart rate fluctuations at the onset of muscular exercise. *J Appl Physiol* 40:679–682
- Farhi LE, Rahn H (1955) A theoretical analysis of the alveolar-arterial  $O_2$  difference, with special reference to the distribution effect. *J Appl Physiol* 7:699–703
- Ferretti G (2012) Da una catastrofe a un modello: la curva di dissociazione dell'ossiemoglobina. *pH* 1: 35–41
- Ferretti G, Boutellier U, Pendergast DR, Moia C, Minetti AE, Howald H, di Prampero PE (1990) Muscular exercise at high altitude. IV. Oxygen transport system before and after exposure to chronic hypoxia. *Int J Sports Med* 11:S15–S20
- Ferretti G, Kayser B, Schena F, Turner DL, Hoppeler H (1992) Regulation of perfusive  $O_2$  transport during exercise in humans: effects of changes in haemoglobin concentration. *J Physiol* 455:679–688
- Ferretti G, Licker MJ, Anchisi S, Moia C, Susta D, Morel DR (2005) The effects of beta1-adrenergic blockade on cardiovascular oxygen flow in normoxic and hypoxic humans at exercise. *Eur J Appl Physiol* 95:250–259
- Ferretti G, Bringard A, Perini R (2011) An analysis of performance in human locomotion. *Eur J Appl Physiol* 111:391–401
- Fick A (1870) Über die Messung des Blutquantums in den Herzventrikeln. *Physikalisch Medizin Gesellschaft, Würzburg*
- Francescato MP, Girardis M, di Prampero PE (1995) Oxygen cost of internal work during cycling. *Eur J Appl Physiol* 72:51–57
- Gaesser GA, Brooks GA (1975) Muscular efficiency during steady-rate exercise: effects of speed and work rate. *J Appl Physiol* 38:1132–1139
- Geppert J, Zuntz N (1888) Über die Regulation der Atmung. *Arch Ges Physiol* 42:189–244
- Girardis M, Linnarsson D, Moia C, Pendergast DR, Ferretti G (1999) Oxygen cost of dynamic leg exercise on a cycle ergometer: effects of gravity acceleration. *Acta Physiol Scand* 166:239–246
- Gonzalez-Alonso J, Richardson RS, Saltin B (2001) Exercising skeletal muscle blood flow in humans responds to reduction in arterial oxyhaemoglobin, but not to altered free oxygen. *J Physiol* 530:331–341
- Gonzalez-Alonso J, Olsen DB, Saltin B (2002) Erythrocyte and the regulation of human skeletal muscle blood flow and oxygen delivery: role of circulating ATP. *Circ Res* 91:1046–1055
- Hagberg JM, Coyle EF (1984) Physiological comparison of competitive race walking and running. *Int J Sports Med* 5:74–77
- Hartley LH, Vogel JA, Landowne L (1973) Central, femoral and brachial circulation during exercise in hypoxia. *J Appl Physiol* 34:87–90
- Heinonen I, Nesterov SV, Kempainen J, Nuutila P, Knuuti J, Laitio R, Kjaer M, Boushel R, Kalliokoski KK (2007) Role of adenosine in regulating the heterogeneity of skeletal muscle blood flow during exercise in humans. *J Appl Physiol* 103:2042–2048
- Heinonen I, Duncker DJ, Knuuti J, Kalliokoski KK (2012) The effect of acute exercise with increasing workloads on inactive muscle blood flow and its heterogeneity in humans. *Eur J Appl Physiol* 112:3503–3509
- Helgerud J (1994) Maximal oxygen uptake, anaerobic threshold and running economy in women and men with similar performances level in marathons. *Eur J Appl Physiol* 68:155–161
- Helgerud J, Storen O, Hoff J (2010) Are there differences in running economy at different velocities for well-trained distance runners? *Eur J Appl Physiol* 108:1099–1105
- Hermansen L, Ekblom B, Saltin B (1970) Cardiac output during submaximal and maximal treadmill and bicycle exercise. *J Appl Physiol* 29:82–86
- Hill AV (1910) The possible effects of the aggregation of the molecules of haemoglobin on its dissociation curves. *J Physiol* 40: iv–vii

- Holmér I (1974) Energy cost of arm stroke, leg kick and the whole stroke in competitive swimming styles. *Eur J Appl Physiol* 33:105–118
- Hughes RL, Clode M, Edwards RH, Goodwin TJ, Jones NL (1968) Effect of inspired O<sub>2</sub> on cardiopulmonary and metabolic responses to exercise in man. *J Appl Physiol* 24:336–347
- Jones AM, Doust JH (1996) A 1 % treadmill grade most accurately reflects the energetic cost of outdoor running. *J Sports Sci* 14:321–327
- Koskolou MD, Calbet JAL, Rådegran G, Roach RC (1997) Hypoxia and cardiovascular response to dynamic knee extensor exercise. *Am J Physiol Heart Circ Physiol* 273:H1787–H1793
- Krogh A (1922) The anatomy and physiology of capillaries. Yale University Press, New Haven
- Lador F, Azabji Kenfack M, Moia C, Cautero M, Morel DR, Capelli C, Ferretti G (2006) Simultaneous determination of the kinetics of cardiac output, systemic O<sub>2</sub> delivery, and lung O<sub>2</sub> uptake at exercise onset in men. *Am J Physiol Regul Integr Comp Physiol* 290:1071–1079
- Léger L, Mercier B (1984) Gross energy cost of horizontal treadmill and track running. *Sports Med* 1:270–277
- Malliani A, Pagani M, Lombardi F, Cerutti S (1991) Cardiovascular neural regulation explored in the frequency domain. *Circulation* 84:482–492
- Marconi C, Heisler N, Meyer M, Weitz H, Pendergast DR, Cerretelli P, Piiper J (1988) Blood flow distribution and its temporal variability in stimulated dog gastrocnemius muscle. *Respir Physiol* 74:1–13
- Margaria R, Cerretelli P, Aghemo P, Sassi G (1963) Energy cost of running. *J Appl Physiol* 18:367–370
- McMiken DF, Daniels JT (1976) Aerobic requirements and maximum aerobic power in treadmill and track running. *Med Sci Sports* 8:14–17
- Minetti AE, Pinkerton J, Zamparo P (2001) From bipedalism to bicyclism: evolution in energetics and biomechanics of historic bicycles. *Proc Roy Soc Lond B* 268:1351–1360
- Minetti AE, Moia C, Roi GS, Susta D, Ferretti G (2002) Energy cost of human locomotion at extreme uphill and downhill slopes. *J Appl Physiol* 93:1039–1046
- Morgan DW, Martin PE, Krahenbuhl GS (1989) Factors affecting running economy. *Sports Med* 7:310–330
- Mortensen SP, Thaning P, Nyberg M, Saltin B, Hellsten Y (2011) Local release of ATP into the arterial inflow and venous drainage of human skeletal muscle: insight from ATP determination with the intravascular microdialysis technique. *J Physiol* 589:1847–1857
- Nadel ER, Cafarelli E, Roberts MF, Wenger CB (1979) Circulatory regulation during exercise in different ambient temperatures. *J Appl Physiol* 46:430–437
- Padilla S, Bourdin M, Barthélémy JC, Lacour JR (1992) Physiological correlates of middle-distance running performance. A comparative study between men and women. *Eur J Appl Physiol* 65:561–566
- Pendergast DR, di Prampero PE, Craig AB Jr, Wilson DR, Rennie DW (1977) Quantitative analysis of the front crawl in men and women. *J Appl Physiol* 43:475–479
- Perini R, Veicsteinas A (2003) Heart rate variability and autonomic activity at rest and during exercise in various physiological conditions. *Eur J Appl Physiol* 90:317–325
- Perutz MF (1970) Stereochemistry of cooperative effects in haemoglobin. *Nature* 228:726–733
- Piiper J, Scheid P (1981) Model for capillary-alveolar equilibration with special reference to O<sub>2</sub> uptake in hypoxia. *Respir Physiol* 46:193–208
- Piiper J, Pendergast DR, Marconi C, Meyer M, Heisler N, Cerretelli P (1985) Blood flow distribution in dog gastrocnemius muscle at rest and during stimulation. *J Appl Physiol* 58:2068–2074
- Pugh LGCE (1970) Oxygen intake in track and treadmill running with observations on the effect of air resistance. *J Physiol Lond* 207:823–835
- Rahn H, Fenn WO (1955) A graphical analysis of the respiratory gas exchange. Am Physiol Soc, Washington DC
- Rennie DW, di Prampero PE, Cerretelli P (1971) Effects of water immersion on cardiac output, heart rate and stroke volume of man at rest and during exercise. *Med Sport Turin* 24:223–228

- Roach RC, Koskolou MD, Calbet JAL, Saltin B (1999) Arterial O<sub>2</sub> content and tension in regulation of cardiac output and leg blood flow during exercise in humans. *Am J Physiol Heart Circ Physiol* 276:H438–H445
- Robinson BF, Epstein SE, Beiser GD, Braunwald E (1966) Control of heart rate by the autonomic nervous system: studies in man on the interrelation between baroreceptor mechanisms and exercise. *Circ Res* 19:400–411
- Roca J, Hogan MC, Story D, Bebout DE, Haab P, Gonzalez R, Ueno O, Wagner PD (1989) Evidence for tissue diffusion limitation of in normal humans. *J Appl Physiol* 67:291–299
- Rowell LB (1974) Human cardiovascular adjustments to exercise and thermal stress. *Physiol Rev* 54:75–159
- Rowell LB, Brengelmann GL, Blackmon JR, Twiss RD, Kusumi F (1968) Disparities between aortic and peripheral pulse pressures induced by upright exercise and vasomotor changes in man. *Circulation* 37:954–964
- Rowell LB, O’Leary DS, Kellogg DL Jr (1996) Integration of cardiovascular control systems in dynamic exercise. In: *Handbook of physiology. Exercise: regulation and integration of multiple systems*, Sect. 12, Chap. 17. Bethesda, MD, pp 770–838 (Am Physiol Soc)
- Saltin B, Blomqvist G, Mitchell JH, Johnson RL, Wildenthal K, Chapman CB (1968) Response to exercise after bed rest and after training. *Circulation* 38(5):1–78
- Seals DR, Victor RG (1991) Regulation of muscle sympathetic nerve activity during exercise in humans. *Exerc Sports Sci Rev* 19:313–349
- Sheldahl LM, Tristani FE, Clifford PS, Hughes CV, Sobocinski KA, Morris RD (1987) Effect of head-out water immersion on cardiorespiratory response to dynamic exercise. *J Am Coll Cardiol* 10:1254–1258
- Stamler JS, Jia L, Eu JP, McMahon TJ, Demchenko IT, Bonaventura J, Gernert K, Piantadosi CA (1997) Blood flow regulation by S-nitrosohemoglobin in the physiological oxygen gradient. *Science* 276:2034–2037
- Stenberg J, Eklblom B, Messin R (1966) Hemodynamic response to work at simulated altitude, 4,000 m. *J Appl Physiol* 21:1589–1594
- Stenberg J, Åstrand PO, Eklblom B, Royce J, Saltin B (1967) Hemodynamic response to work with different muscle groups, sitting and supine. *J Appl Physiol* 22:61–70
- Stickland MK, Fuhr DP, Haykowsky MJ, Jones KE, Paterson DI, Ezekowitz JA, McMurtry MS (2011) Carotid chemoreceptor modulation of blood flow during exercise in healthy humans. *J Physiol* 589:6219–6230
- Tam E, Rossi H, Moia C, Berardelli C, Rosa G, Capelli C, Ferretti G (2012) Energetics of running in top-level marathon runners from Kenya. *Eur J Appl Physiol* 112:3797–3806
- Tanabe N, Todoran TM, Zenk GM, Bunton BR, Wagner WW, Presson RG (1998) Perfusion heterogeneity in the pulmonary acinus. *J Appl Physiol* 84:933–938
- Termin B, Pendergast DR (2000) Training using the stroke frequency—velocity relationship to combine biomechanical and metabolic paradigms. *J Swim Res* 14:9–17
- Vogel JA, Gleser MA (1972) Effect of carbon monoxide on oxygen transport during exercise. *J Appl Physiol* 32:234–239
- Wagner PD, West JB (1972) Effects of diffusion impairment on O<sub>2</sub>, and CO<sub>2</sub> time courses in pulmonary capillaries. *J Appl Physiol* 33:62–71
- Woodson RD, Wills RE, Lenfant C (1978) Effect of acute and established anemia on O<sub>2</sub> transport at rest, submaximal and maximal work. *J Appl Physiol* 44:36–43
- Zamparo P, Pendergast DR, Termin AB, Minetti AE (2002) How fins affect the economy and efficiency of human swimming. *J Exp Biol* 205:2665–2676
- Zamparo P, Lazzar S, Antoniazzi C, Cedolin S, Avon R, Lesa C (2008) The interplay between propelling efficiency, hydrodynamic position and energy cost of front crawl in 8 to 19-year-old swimmers. *Eur J Appl Physiol* 104:689–699
- Zamparo P, Gatta G, Capelli C, Pendergast DR (2009) Active and passive drag, the role of trunk incline. *Eur J Appl Physiol* 106:195–205
- Zamparo P, Capelli C, Pendergast DR (2011) Energetics of swimming: a historical perspective. *Eur J Appl Physiol* 111:367–378

Energetics of Muscular Exercise

Ferretti, G.

2015, XXII, 180 p. 47 illus., 20 illus. in color., Hardcover

ISBN: 978-3-319-05635-7